Eur. Phys. J. E **17**, 261–281 (2005)
DOI 10.1140/epje/i2005-10013-y

THE EUROPEAN PHYSICAL JOURNAL E

Crack motion in viscoelastic solids: The role of the flash temperature

G. Carbone[1,2,3,a] and B.N.J. Persson[2]

[1] DIMeG-Politecnico di Bari, V.le Japigia 182, 70126 Bari, Italy
[2] IFF Forschungszentrum Jülich, 52425 Jülich, Germany
[3] CEMeC-Politecnico di Bari, Via Re David 200, 70125, Bari, Italy

Received 28 January 2005 /
Published online: 5 July 2005 –

Abstract. We present a simple theory of crack propagation in viscoelastic solids. We calculate the energy per unit area, $G(v)$, to propagate a crack, as a function of the crack tip velocity v. Our study includes the non-uniform temperature distribution (flash temperature) in the vicinity of the crack tip, which has a profound influence on $G(v)$. At very low crack tip velocities, the heat produced at the crack tip can diffuse away, resulting in very small temperature increase: in this "low-speed" regime the flash temperature effect is unimportant. However, because of the low heat conductivity of rubber-like materials, already at moderate crack tip velocities a very large temperature increase (of order of 1000 K) can occur close to the crack tip. We show that this will drastically affect the viscoelastic energy dissipation close to the crack tip, resulting in a "hot-crack" propagation regime. The transition between the low-speed regime and the hot-crack regime is very abrupt, which may result in unstable crack motion, *e.g.* stick-slip motion or catastrophic failure, as observed in some experiments. In addition, the high crack tip temperature may result in significant thermal decomposition within the heated region, resulting in a liquid-like region in the vicinity of the crack tip. This may explain the change in surface morphology (from rough to smooth surfaces) which is observed as the crack tip velocity is increased above the instability threshold.

PACS. 46.50.+a Fracture mechanics, fatigue and cracks – 83.60.Bc Linear viscoelasticity – 46.55.+d Tribology and mechanical contacts

1 Introduction

The propagation of cracks in rubber is fundamental for many important applications, *e.g.*, rubber wear [1], for pressure sensitive adhesives [2], and also for sliding or rolling friction on smooth substrates [3]. The strength of adhesion and cohesion of elastomers can be characterized by the amount of energy G required to advance the crack tip by one unit area. Experiments have shown that G depends on the crack tip velocity v and on the temperature T and that [4–6]

$$G(v,T) = G_0\left[1 + f(v,T)\right] , \qquad (1)$$

where $f \to 0$ as $v \to 0$. Thus, G_0 is a threshold value below which no fracture occurs. The measured value of G at extremely low crack velocities and high temperatures, when viscous effects in the rubber are minimized, is of order $\sim 1\,\mathrm{eV/\AA^2}$ and can be identified as G_0. For simple hydrocarbon elastomers, the effect of temperature can be completely accounted for by applying a simple multiplying factor, denoted by a_T, to the crack velocity v, *i.e.*, $f(v,T) = f(a_T v)$. Moreover, values of a_T determined experimentally are equal to the Williams-Landel-Ferry [7] function determined from the temperature dependence of the bulk viscoelastic modulus. This clearly proves that the large effects of crack velocity and temperature on crack propagation in rubber materials are due to viscoelastic processes in the bulk.

In order to understand the physical origin of expression (1) it is necessary to know the general structure of the viscoelastic modulus $E(\omega)$ of rubber-like materials. In Figure 1 we show the real $E_1 = \mathrm{Re}E$ and the imaginary part $E_2 = \mathrm{Im}E$ of $E(\omega)$ and also the loss tangent E_2/E_1. At "low" frequencies the material is in the "rubbery" region, where $\mathrm{Re}E(\omega)$ is relative small and approximately constant. At very high frequencies the material is elastically very stiff (brittle-like). In this "glassy" region $\mathrm{Re}E$ is again nearly constant but much larger (typically by 3 to 4 orders of magnitude) than in the rubbery region. In the intermediate frequency range (the "transition" region) the loss tangent is very large and it is mainly this region

[a] e-mail: carbone@poliba.it

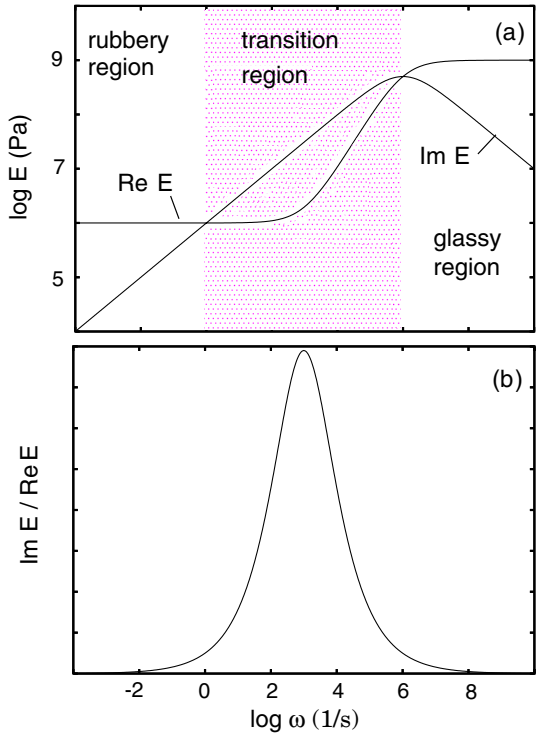

Fig. 1. (a) The viscoelastic modulus $E(\omega) = E_1 + iE_2$ of a typical rubber-like material, and (b) the loss tangent E_2/E_1. The latter quantity is maximal at some frequency ω_2. (Schematic.)

which determines, *e.g.*, the friction when a tire is sliding on a road surface [8]. In what follows we will refer to the peak in the loss tangent curve (see Fig. 2(b)) as the viscoelastic loss peak.

The physical origin of the dynamical modulus $E(\omega)$ for rubber-like materials is related to stress-aided, thermally activated flipping of polymer segments between different configurations. If τ denotes the typical flipping time, then for $\omega \gg 1/\tau$ there is no time for thermally activated rearrangement of the polymer chain segments to occur, and the rubber response will be that of a hard glassy material. However, when $\omega \ll 1/\tau$, thermal activated rearrangements of the rubber polymer chains will occur adiabatically, resulting in a soft rubbery response. In fact, $E(\omega, T)$ will be a function of the form $E = E(\omega\tau)$, where τ depends on temperature according to a thermally activated process. Usually, one writes $\tau = \tau_0 a_T$, where τ_0 is temperature independent, and where a_T is (approximately) given by the WLF function proposed by Williams, Landel and Ferry [7]:

$$\log\, a_T = \frac{C_1(T - T_{\rm g})}{C_2 + T - T_{\rm g}}\,,$$

where C_1 and C_2 are two constants and where $T_{\rm g}$ is the glass transition temperature of the rubber.

The energy dissipation at a crack in a viscoelastic solid has two contributions, see Figure 2. The first is associated with the most inner region at the crack tip (the so-called crack tip process zone; the dark area at the crack tip in Fig. 2), and involves highly non-linear processes (*e.g.*, cavity formation, stringing, chain pull-out (for polymers), and bond-breaking) and is described phenomenologically via the term $G_0 = 2\gamma_0$. (Note: for rubber-like materials γ_0 is much larger than the surface energy γ.) This contribution to $G(v)$ cannot be accurately calculated theoretically, and is taken as an input (determined experimentally) in the theory. The second contribution (described by the factor $f(v, T)$) comes from the viscoelastic dissipation in the polymer in the linear viscoelastic region in front of the tip. If the *loss function* $\mathrm{Im}[1/E(\omega)]$ is maximal at some characteristic frequency ω_1, then this dissipative region will be centered a distance $r \sim v/\omega_1$ from the crack tip. For a fast moving crack this may be very far away from the crack tip. This contribution is calculated by the theory [9–14], and it has recently been shown [14] that the exact form of the crack tip process zone is not important for the calculation of the viscoelastic contribution to G. The strongest velocity dependence in (1) is derived from the factor $f(v, T)$ which at high crack tip velocities may enhance G by a factor 10^3 or more.

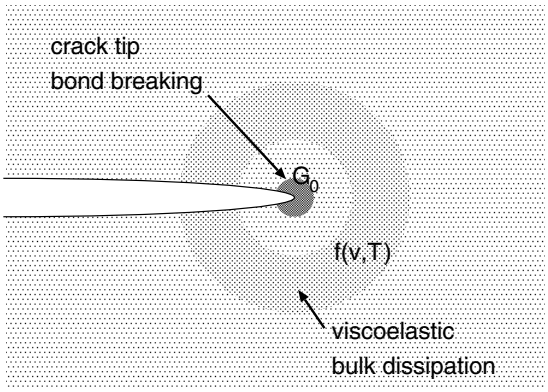

Fig. 2. The crack propagation energy G is a product of a term G_0 derived from the bond-breaking at the crack tip, and a term $f(v, T)$ derived from the bulk viscoelastic energy dissipation in front of the tip.

In this article we discuss the nature of G for viscoelastic solids. The results presented below are based on the energy-balance approach to crack propagation. In this approach one first calculates the viscoelastic energy dissipation in the vicinity of a crack tip, and then uses it to derive a general expression for $G(v) = 2\gamma_{\rm eff}(v)$. This approach is much simpler than the treatment presented in most earlier studies, and under isothermal conditions it results in a simple analytical formula for $G(v)$ [14]. Furthermore, as we will show in this paper, the theory can be generalized to include the influence of the tip flash temperature on the crack propagation.

The standard model used to describe the crack tip process zone is due to Barenblatt [15]. He assumed that the bond-breaking at the crack tip occurs by stretching the bonds orthogonal to the crack surfaces until they break at some characteristic stress level σ_c. The process zone extends a distance a in front of the crack tip. This model was first applied to crack propagation in viscoelastic solids by Schapery [10] and later by Greenwood and Johnson [11],

Barber *et al.* [12], and by Hui *et al.* [13]. In reference [14] a simpler treatment was presented, where the cut-off was introduced in a more *ad hoc* manner, which may be roughly interpreted as a blunting of the crack. It was also shown that the exact way the cut-off is introduced is unimportant, and in reality the process zone is much more complex than assumed in the theory. In general, the cut-off should be introduced in such a way as to simplify the analytical calculations as much as possible, and for crack propagation in viscoelastic solids we believe that the cut-off procedure used in reference [14] and in the present paper results in the simplest formalism.

Very recently it has been observed that propagating cracks in viscoelastic materials, such as tyre rubber, sometimes exhibit unstable stick-slip behavior [16–18], or catastrophic fracture [16]. In this paper we show that unstable crack propagation may result when the non-uniform temperature distribution (flash temperature), which occurs in the vicinity of the crack tip, is taken into account. The strong dependence of the crack dynamics on the flash temperature results from the extreme temperature sensitivity of the viscoelastic modulus $E(\omega)$ for rubber-like materials. We show that because of the flash temperature the function $G(v)$ does not have a monotonic behavior, which may result in unstable crack propagation when the (average) crack propagation speed is in some well-defined velocity range. This situation is very similar to rubber friction on rough substrates, where the flash temperature gives rise to a decreasing rubber friction coefficient for sliding velocities above $\sim 1\,\mathrm{cm/s}$; this in turn may give rise to stick-slip motion [19].

In a previous paper one of the authors (BP) has developed a simple theory for the energy $G(v)$ per unit area needed to propagate a crack in a viscoelastic solid [14]. This theory is in good agreement with experiments performed at very low crack speed, where the temperature increase in the rubber can be neglected, but the theory cannot explain crack propagation instabilities, which we believe are related to the non-uniform crack tip temperature distribution. In this paper we extend the theory in reference [14] to include the crack tip flash temperature which, because of the low heat conductivity of rubber-like materials, turns out to be extremely important already at relative low crack propagation velocities.

This paper is organized as follows. In Section 2 we present a simple estimate which shows the crucial role of the crack tip flash temperature on crack propagation in rubber-like materials. In Section 3 we briefly consider crack propagation in elastic solids. In Section 4 we calculate the (bulk) viscoelastic energy dissipation in front of the crack tip for a linear viscoelastic solid, under isothermal condition. In Section 5 we present the basic theory for the non-uniform crack tip temperature distribution and the crack propagation energy G. Sections 6 and 7 present numerical results for the Kelvin model and for a more general viscoelastic model, respectively. In Section 8 we discuss how the high temperature at the crack tip may result in a thermally degraded layer at the crack tip, and we study how this may influence the crack propagation energy G. In Section 9 we explain (qualitatively) how some of the results of the calculations can be understood based on a very simple model. In Section 10 we compare the theory with experiments. The theory presented in this paper assumes that inertia effects can be neglected. This is the case for cracks which moves much slower than the sound velocity in the solid. In Section 11 we briefly discuss how the theory is modified at highly crack propagation velocities, where inertia effects becomes important. Section 12 presents a general discussion about different models used for the crack tip process zone, and how it affects the crack propagation energy G_0. The conclusions are presented in Section 13.

2 Crack tip flash temperature: Qualitative discussion

In this paper we will demonstrate the fundamental importance of the non-uniform temperature distribution (flash temperature) at the crack tip. It is easy to show that the temperature increase at the crack tip may be very high. The crack propagation energy per unit created surface area, for a crack propagating in rubber at the velocity $\sim 10\,\mathrm{cm/s}$, is typically $G \approx 10^4\,\mathrm{J/m^2}$ ($\approx 10^3\,\mathrm{eV/\AA^2}$). Most of the energy dissipation occurs at a typical distance from the crack tip given by $r \sim v/\omega_1$, where v is the crack tip velocity and ω_1 is the frequency for which $\mathrm{Im}[1/E(\omega)]$ is maximal (which is related to the frequency ω_2 of the maximum of the loss tangent $\mathrm{Im}E(\omega)/\mathrm{Re}E(\omega)$ via $\omega_1 \approx (E_0/E_\infty)^{1/2}\omega_2$, where E_0 and E_∞ are the zero-frequency and high-frequency elastic modulus, respectively) (this result is only valid as long as $v/\omega_1 > a(v)$, where $a(v)$ is the crack tip radius defined in Sect. 4). For the styrene-butadiene copolymer at room temperature $\omega_1 \approx 10^4\,\mathrm{s^{-1}}$ and if $v = 10\,\mathrm{cm/s}$, we get $r \approx 10\,\mu\mathrm{m}$. On the time scale $\sim \tau = r/v \approx 10^{-4}\,\mathrm{s}$ and the length scale $\sim r$, heat diffusion is negligible since $D\tau/r^2 \approx 0.1 \ll 1$, where the heat diffusivity $D = \lambda/\rho C_V \approx 10^{-7}\,\mathrm{m^2/s}$ ($\rho \approx 1200\,\mathrm{kg/m^3}$ is the mass density, $\lambda \approx 0.15\,\mathrm{W/mK}$ the heat conductivity and $C_V \approx 1400\,\mathrm{J/kgK}$ the heat capacity). Thus, the temperature increase at the crack tip can be estimated using $\rho C_V \Delta T \approx G/r$ or $\Delta T \approx G/(\rho C_V r) \approx 10^3\,\mathrm{K}$. Note also that for $v \ll v_c$ the temperature increase will be negligible, there v_c is determined by the condition $D\tau/r^2 \approx 1$. Using that $\tau = 1/\omega_1$ and $r = v_c\tau$ gives $D\omega_1/v_c^2 = 1$ so that $v_c = (D\omega_1)^{1/2} \approx 3\,\mathrm{cm/s}$.

The high temperatures at the crack tip when the crack velocity $v > v_c$ will result in thermal degradation of the rubber in the vicinity of the crack tip. Roughly speaking, the rubber will "melt" in a small region at the crack tip. We believe that this is the reason why smooth crack surfaces are observed for large crack tip velocities [18]. For low crack tip velocities $v \ll v_c$ the crack surfaces are instead very rough, as is typically observed during fracture of brittle solids.

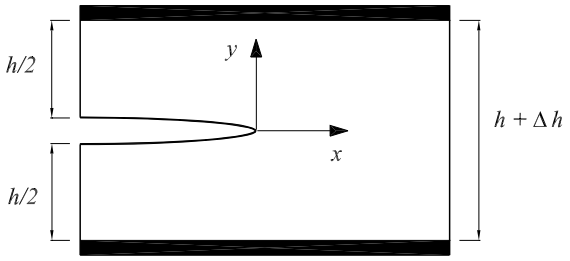

Fig. 3. A crack in an infinitely long (in the x-direction) elastic plate. The upper and lower surfaces are clamped in the perpendicular direction (but free to slip in the parallel direction), and separated by a distance Δh.

3 Crack in elastic solid

Consider an elastic slab with width h, and assume that it contains a semi-infinite crack as illustrated in Figure 3. Assume that the solid boundaries at $y = \pm h/2$ are displaced by a distance Δh, while they are free to slip within the xz-plane. This will result in a plain stress situation. We can obtain the crack equilibrium condition for an ideal elastic material by simply equating the gain of surface energy per unit thickness, due to a (forward) displacement δx of the crack tip, to the change of the elastic energy per unit thickness stored in the solid. We have

$$\delta U_{\rm surf} = 2\gamma \delta x, \tag{2}$$

where the quantity γ is the surface energy and the factor 2 is necessary since two surfaces are created, and

$$-\delta U_{\rm el} = \frac{1}{2E} h \sigma_0^2 \delta x. \tag{3}$$

The stress $\sigma_0 = E\varepsilon_0$, where the strain $\varepsilon_0 = \Delta h/h$, and where E is the elastic modulus of the solid. Equating $\delta U_{\rm surf} = -\delta U_{\rm el}$ gives

$$\sigma_0 = \left(\frac{4E\gamma}{h}\right)^{1/2}, \tag{4}$$

which is the classic Griffith criterion [20] for the equilibrium of a crack. For an ideal crack, the *crack propagation energy* (per unit surface area) is $G = 2\gamma$. In an elastic solid the stress tensor close to a crack tip takes the universal form

$$\sigma_{ij} \approx \frac{K}{(2\pi r)^{1/2}} f_{ij}(\phi)\,,$$

where r is the distance from the crack tip [21], and where $f_{ij}(\phi)$ depends on the polar angle ϕ in the xy-plane. For plane stress conditions the *stress intensity factor* K is related to G through the relation $K^2 = GE = 2\gamma E$. Using this equation and (4) we can also write

$$\sigma_{ij} \approx \frac{\sigma_0}{2}\left(\frac{h}{\pi r}\right)^{1/2} f_{ij}(\phi)\,.$$

4 Crack propagation in viscoelastic solids

In viscoelastic solids the energy balance equation must include the energy dissipation in the solid. Let us now calculate the energy dissipation per unit time and unit thickness, P, when a crack propagates with constant velocity $\mathbf{v} = (v_x, 0)$ in a linear viscoelastic solid. Consider first isothermal conditions. In Appendix A we calculate the energy dissipation per unit time and unit thickness for a linear viscoelastic solid subjected to a stress field $\sigma_{ij}(\mathbf{x} - \mathbf{v}t)$ which moves with velocity $\mathbf{v}$:

$$P = (2\pi)^2 \int {\rm d}^2 q \,(-i\mathbf{q}\cdot\mathbf{v})\, C_{ijkh}(\mathbf{q}\cdot\mathbf{v})\, \sigma_{ij}(-\mathbf{q})\, \sigma_{kh}(\mathbf{q})\,. \tag{5}$$

The tensor $C_{ijkh}(\omega)$ is the complex compliance defined as $C_{ijkh}(\omega) = [E_{ijkh}(\omega)]^{-1}$, and $E_{ijkh}(\omega)$ is the complex elastic modulus of the material. In our case the stress tensor close to the crack tip is independent of the detailed relation between the stress and strain (*i.e.*, also valid for a viscoelastic material) and takes the universal form (see App. B)

$$\sigma(\mathbf{x} - \mathbf{v}t) \approx \frac{\sigma_0}{2}\left(\frac{h}{\pi|\mathbf{x} - \mathbf{v}t|}\right)^{1/2}. \tag{6}$$

Here we have neglected the tensorial character of the stress field which enters via a function $f_{ij}(\phi)$. However, later we will correct for this. In this case we can write

$$\sigma(\mathbf{q}, t) = e^{-i\mathbf{q}\cdot\mathbf{v}t}\sigma(\mathbf{q})\,, \tag{7}$$

where

$$\sigma(\mathbf{q}) = \frac{1}{(2\pi)^2}\int {\rm d}^2 x\; \sigma(\mathbf{x})\, e^{-i\mathbf{q}\cdot\mathbf{x}} = \frac{h^{1/2}\sigma_0}{4\pi\sqrt{\pi}} q^{-3/2}\int_0^\infty {\rm d}w\; w^{1/2} J_0(w)\,. \tag{8}$$

Here

$$\int_0^\infty {\rm d}w\; w^{1/2} J_0(w) = \sqrt{2}\frac{\Gamma(3/4)}{\Gamma(1/4)} = \alpha' \tag{9}$$

is a number of order unity ($\alpha' \approx 0.48$) and Γ is the gamma function. However, in the above calculations we have neglected the angular dependence of the stress field. In order to account for this angular dependence we replace α' with $\alpha^{1/2}$ and write

$$\sigma(\mathbf{q}) = \frac{\alpha^{1/2} h^{1/2}\sigma_0}{4\pi\sqrt{\pi}} q^{-3/2} = \sigma(q)\,, \tag{10}$$

where α is a number of order unity which we will determine below. Having determined $\sigma(\mathbf{q})$, and neglecting the tensorial character of the stress field, the energy dissipation per unit time and unit thickness can be calculated

from (5):

$$P = (2\pi)^2 \int \mathrm{d}^2q \frac{-i\mathbf{q}\cdot\mathbf{v}}{E\left(\mathbf{q}\cdot\mathbf{v}\right)} \left|\sigma\left(q\right)\right|^2 = (2\pi)^2 \int \mathrm{d}\omega \mathrm{d}^2q \left|\sigma\left(q\right)\right|^2 \delta\left(\omega + \mathbf{q}\cdot\mathbf{v}\right) \frac{i\omega}{E\left(-\omega\right)} = (2\pi)^2 \int \mathrm{d}\omega \int_0^\infty \mathrm{d}qq \left|\sigma\left(q\right)\right|^2 \frac{i\omega}{E\left(-\omega\right)} \times \int_0^{2\pi} \mathrm{d}\phi \delta\left(\omega + qv\cos\phi\right) . \quad (11)$$

Now observe that

$$\int_0^{2\pi} \mathrm{d}\phi \delta\left(\omega + qv\cos\phi\right) = 2\frac{\theta\left(q^2v^2 - \omega^2\right)}{\left[\left(qv\right)^2 - \omega^2\right]^{1/2}}, \quad (12)$$

where $\theta\left(x\right)$ is the Heaviside unit step function. Thus the energy dissipation P can be written as

$$P = 8\pi^2 \int \mathrm{d}\omega \int_0^\infty \mathrm{d}qq \left|\sigma\left(q\right)\right|^2 \frac{i\omega}{E\left(-\omega\right)} \frac{\theta\left(q^2v^2 - \omega^2\right)}{\left[\left(qv\right)^2 - \omega^2\right]^{1/2}} = 16\pi^2 \int_0^\infty \mathrm{d}\omega \,\mathrm{Im}\left[\frac{\omega}{E\left(\omega\right)}\right] \times \int_{\omega/v}^\infty \mathrm{d}qq \left|\sigma\left(q\right)\right|^2 \left(q^2v^2 - \omega^2\right)^{-1/2} . \quad (13)$$

Using (10) we finally obtain

$$P = \frac{1}{\pi}\alpha\sigma_0^2 h \int_0^{\omega_c} \mathrm{d}\omega\omega \int_{\omega/v}^{q_c} \mathrm{d}qq^{-2} \left(q^2v^2 - \omega^2\right)^{-1/2} \times \mathrm{Im}\frac{1}{E\left(\omega, T_0\right)} . \quad (14)$$

In (14) we have introduced the large cut-off wave vector $q_c = 2\pi/a$, and the corresponding large cut-off frequency $\omega_c = 2\pi v/a$, where a is taken equal to the radius of the crack tip. In (14) we also indicate explicitly that the viscoelastic modulus depends on the temperature T, which in the analysis above was assumed to be constant, $T = T_0$.

5 Non-uniform temperature distribution: Basic theory

Until now we have neglected the fact that the viscoelastic energy dissipation in front of the crack produces heating. The resulting temperature increase can have a large influence on the energy dissipation because of the extreme sensitivity of the viscoelastic modulus $E(\omega, T)$ on the temperature. The temperature distribution is not uniform, and this must be taken into account when calculating the viscoelastic energy dissipation. The simplest approach is still to use (14), but replacing the viscoelastic modulus $E(\omega, T_0)$ with $E(\omega, T_q)$, where T_q is the temperature in the spatial region in front of the crack tip probed by the q-wave number contribution to the integral (14). Thus, (14) is replaced by

$$P = \frac{1}{\pi}\alpha\sigma_0^2 h \int_0^{\omega_c} \mathrm{d}\omega\omega \int_{\omega/v}^{q_c} \mathrm{d}qq^{-2} \left(q^2v^2 - \omega^2\right)^{-1/2} \times \mathrm{Im}\frac{1}{E\left(\omega, T_q\right)} . \quad (15)$$

5.1 Effective energy required to propagate the crack

In the present case the elastic energy stored in a vertical slab in front of the crack tip is partially used to break the bonds at the crack tip, described by $G_0 = 2\gamma_0$, and the rest is dissipated via the internal friction in the rubber according to (15). It follows that

$$-\frac{\mathrm{d}U_{\mathrm{el}}}{\mathrm{d}t} = \frac{\mathrm{d}U_{\mathrm{surf}}}{\mathrm{d}t} + P. \quad (16)$$

Observe that far form the crack tip the material is fully relaxed and the elastic modulus is that corresponding to the zero frequency $E\left(0\right) = E_0$. Thus, the rate of change of elastic energy per unit thickness is $\mathrm{d}U_{\mathrm{el}}/\mathrm{d}t = -\sigma_0^2 hv/2E_0$, whereas the rate of change of the adhesion or cohesion energy is $\mathrm{d}U_{\mathrm{surf}}/\mathrm{d}t = 2\gamma_0 v$. Substituting these results and (15) into (16) gives

$$\frac{\sigma_0^2 h}{2E_0}v = 2\gamma_0 v + \frac{1}{\pi}\alpha\sigma_0^2 h \int_0^{\omega_c} \mathrm{d}\omega\omega \int_{\omega/v}^{q_c} \mathrm{d}qq^{-2} \times \left(q^2v^2 - \omega^2\right)^{-1/2} \mathrm{Im}\frac{1}{E\left(\omega, T_q\right)} . \quad (17)$$

We define the effective energy to propagate the crack

$$G = 2\gamma_{\mathrm{eff}} = \frac{\sigma_0^2 h}{2E_0} . \quad (18)$$

Using this definition and defining $q = yq_c$ and $\omega = x\omega_c$, we obtain from (17)

$$\frac{\gamma_{\mathrm{eff}}}{\gamma_0} = \left[1 - \frac{2}{\pi}\alpha \int_0^1 \mathrm{d}xx \int_x^1 \mathrm{d}yy^{-2} \left(y^2 - x^2\right)^{-1/2} \times \mathrm{Im}\frac{E_0}{E\left(x\omega_c, T_y\right)}\right]^{-1} \quad (19)$$

where T_y stands for T_q with $q = yq_c$.

We can calculate the factor α by observing that for very high crack velocities (see App. C, and also Refs. [9, 14, 22, 23])

$$\frac{\gamma_{\mathrm{eff}}}{\gamma_0} = \frac{E_\infty}{E_0}. \quad (20)$$

Equation (20) can be used to show that $\alpha = 1$. First, note the *sum rule* (see App. D):

$$\frac{1}{E_0} - \frac{1}{E_\infty} = \frac{2}{\pi}\int_0^\infty \mathrm{d}\omega \,\frac{1}{\omega}\mathrm{Im}\frac{1}{E(\omega)} . \quad (21)$$

Now, as $v \to \infty$ we have $\omega_c \to \infty$. Thus,

$$\int_0^1 \mathrm{d}x x \int_x^1 \mathrm{d}y y^{-2} \left(y^2 - x^2\right)^{-1/2} \mathrm{Im}\, \frac{1}{E\left(x\omega_c\right)} \to \int_0^\infty \mathrm{d}\omega \frac{1}{\omega} \mathrm{Im}\, \frac{1}{E\left(\omega\right)} = \frac{\pi}{2}\left(\frac{1}{E_0} - \frac{1}{E_\infty}\right). \quad (22)$$

From equations (19), (20) and (22) we get $\alpha = 1$ and

$$\frac{\gamma_{\mathrm{eff}}}{\gamma_0} = \left[1 - \frac{2}{\pi}\int_0^1 \mathrm{d}x x \int_x^1 \mathrm{d}y y^{-2}\left(y^2 - x^2\right)^{-1/2} \times \mathrm{Im}\, \frac{E_0}{E\left(x\omega_c, T_y\right)}\right]^{-1}. \quad (23)$$

5.2 Crack tip radius

The radius of curvature of the crack tip a can be calculated by considering that in order for the crack to propagate the stress at the crack tip must be equal to some characteristic (material dependent) yield stress σ_c. Using (6), with σ replaced by σ_c and $|\mathbf{x} - \mathbf{v}t|$ by a, leads to the relation

$$4\pi\sigma_c^2 a = \sigma_0^2 h. \quad (24)$$

From (18) and (24) one obtains

$$\sigma_c^2 a = E_0 \gamma_{\mathrm{eff}}/\pi, \quad (25)$$

which shows that the crack tip radius is proportional to the effective energy γ_{eff} necessary to propagate the crack. We define a reference radius $a_0 = E_0\gamma_0/\left(\pi\sigma_c^2\right)$. This can be interpreted as the crack tip radius for an arbitrary slowly moving crack. Thomas [24] has suggested that a_0 is of order the unstrained distance between the ends of a representative network stand, which typically is of order $a_0 \approx$ 1–10 nm. Using (23) and (25) we get

$$\frac{a}{a_0} = \left[1 - \frac{2}{\pi}\int_0^1 \mathrm{d}x x \int_x^1 \mathrm{d}y y^{-2}\left(y^2 - x^2\right)^{-1/2} \times \mathrm{Im}\, \frac{E_0}{E\left(x\omega_c, T_y\right)}\right]^{-1}. \quad (26)$$

Since ω_c (and the temperature field T_y) depends on the crack tip radius a, this is an implicit equation for a.

5.3 Temperature distribution

We determine T_q from the temperature field $T(\mathbf{x}, t)$ as follows [25]. The temperature field $T(\mathbf{x}, t)$ satisfies the diffusion equation

$$\frac{\partial T}{\partial t} - D\nabla^2 T = \frac{\dot{Q}\left(\mathbf{x}, t\right)}{\rho C_V}, \quad (27)$$

where $\dot{Q}$ is the energy production per unit volume and unit time as a result of the internal friction of the rubber. The heat diffusivity $D = \lambda/\rho C_V$, ρ is the mass density, λ the heat conductivity, and C_V the heat capacity per unit mass. In the present paper we neglect the temperature dependence of the diffusivity D as it is much weaker than for the viscoelastic modulus. Let $\Phi_q(\mathbf{x})$ be a function normalized so that

$$\int \mathrm{d}^2x\ \Phi_q\left(\mathbf{x}\right) = 1. \quad (28)$$

The function Φ_q is chosen to be "large" in the spatial region where most of the energy dissipation occur when we consider the q-wave number contribution to the integral (26), and "small" elsewhere. We then define

$$T_q = \int \mathrm{d}^2x\ \Phi_q\left(\mathbf{x}\right) T\left(\mathbf{x}\right). \quad (29)$$

The simplest possible Φ_q can be obtained by means of dimensional arguments:

$$\Phi_q\left(\mathbf{x}\right) = \frac{q}{2\pi}\delta\left(r - \frac{1}{q}\right), \quad (30)$$

so that

$$T_q = \frac{1}{2\pi}\int \mathrm{d}\phi T\left(\frac{\cos\phi}{q}, \frac{\sin\phi}{q}\right). \quad (31)$$

Therefore, T_q is the angular average of $T(\mathbf{x})$ calculated at a distance $r = 1/q$.

It is not easy to estimate exactly how accurate the approximation (28–30) is. We have used a similar approximation before for rubber friction (unpublished), where good agreement with experimental data was obtained. However, the topic we study is extremely complex (which explains why no earlier analytical studies of the temperature effects has been published), and our treatment is a first analysis aimed at getting some understanding of this problem. Since the results presented below makes physical sense and can be understood in a qualitative way (see Sect. 9), and can be correlated with experimental data, we believe that (28–30) represent a useful way of including a non-uniform temperature distribution in the theory.

For a crack moving with a constant velocity $\mathbf{v}$ we have

$$\dot{Q}(\mathbf{x}, t) = f(\mathbf{x} - \mathbf{v}t). \quad (32)$$

Defining the Fourier transform

$$f(\mathbf{x}) = \int \mathrm{d}^2q\ f(\mathbf{q}) e^{i\mathbf{q}\cdot\mathbf{x}}, \quad (33)$$

we get from (27)

$$T(\mathbf{x}, t) = T_0 + \frac{1}{\rho C_V}\int \mathrm{d}^2q\ \frac{f(\mathbf{q})}{-i\mathbf{q}\cdot\mathbf{v} + Dq^2} e^{i\mathbf{q}\cdot(\mathbf{x} - \mathbf{v}t)}. \quad (34)$$

Thus,

$$T_q = T_0 + \frac{(2\pi)^2}{\rho C_V}\int \mathrm{d}^2p\ \frac{f(\mathbf{p})\Phi_q(-\mathbf{p})}{-i\mathbf{p}\cdot\mathbf{v} + Dp^2}, \quad (35)$$

where

$$\Phi_q(\mathbf{p}) = \frac{1}{(2\pi)^2}\int \mathrm{d}^2x\ \Phi_q(\mathbf{x}) e^{-i\mathbf{p}\cdot\mathbf{x}} = \frac{1}{(2\pi)^2} J_0\left(p/q\right). \quad (36)$$

In order to calculate T_q we must calculate the energy production per unit volume and unit time $f(\mathbf{x})$. We have

$$\dot{Q}(\mathbf{x},t) = f(\mathbf{x}-\mathbf{v}t) = \dot{\varepsilon}\sigma = \int \mathrm{d}\omega\mathrm{d}\omega' \left(-i\omega\right) \frac{\sigma(\mathbf{x},\omega)\,\sigma(\mathbf{x},\omega')}{E(\omega)} e^{-i(\omega+\omega')t} \quad (37)$$

and using that

$$\sigma(\mathbf{x},\omega) = \int \mathrm{d}^2q\delta(\omega-\mathbf{q}\cdot\mathbf{v})\,\sigma(\mathbf{q})\,e^{i\mathbf{q}\cdot\mathbf{x}}, \quad (38)$$

we get

$$\dot{Q}(\mathbf{x},t) = f(\mathbf{x}-\mathbf{v}t) = \int \mathrm{d}^2q\mathrm{d}^2q'\left(-i\mathbf{q}\cdot\mathbf{v}\right) \times \frac{\sigma(\mathbf{q})\,\sigma(\mathbf{q}')}{E(\mathbf{q}\cdot\mathbf{v},T_q)} e^{i(\mathbf{q}+\mathbf{q}')\cdot(\mathbf{x}-\mathbf{v}t)} \quad (39)$$

and

$$f(\mathbf{x}) = \int \mathrm{d}^2q\mathrm{d}^2q'\left(-i\mathbf{q}'\cdot\mathbf{v}\right) \frac{\sigma(\mathbf{q})\,\sigma(\mathbf{q}')}{E(\mathbf{q}'\cdot\mathbf{v},T_{q'})} e^{i(\mathbf{q}+\mathbf{q}')\cdot\mathbf{x}}. \quad (40)$$

Now, since $\sigma(\mathbf{q}) = \sigma(q)$ only depends on $q = |\mathbf{q}|$, equation (40) can be rewritten as

$$f(\mathbf{x}) = 2\pi \int \mathrm{d}q\mathrm{d}^2q'q\left(-i\mathbf{q}'\cdot\mathbf{v}\right) \frac{\sigma(q)\,\sigma(q')}{E(\mathbf{q}'\cdot\mathbf{v},T_{q'})} e^{i\mathbf{q}'\cdot\mathbf{x}} J_0(qr). \quad (41)$$

The angular dependence of the stress field is neglected in the paper, and also the weight function $\Phi_q(\mathbf{x})$ has been chosen to be angular independent. Similarly, instead of $f(\mathbf{x})$ we can use its angular average:

$$\bar{f}(r) = \frac{1}{2\pi}\int_0^{2\pi} f(\mathbf{x})\,\mathrm{d}\phi = \frac{1}{2\pi}\int_0^{2\pi} f(r,\phi)\,\mathrm{d}\phi = 2\pi \int \mathrm{d}\omega\mathrm{d}q\mathrm{d}q'\; qq'\sigma(q)\,\sigma(q')\,J_0(qr)\,J_0(q'r) \times \frac{i\omega}{E(-\omega,T_{q'})} \int_0^{2\pi} \mathrm{d}\phi'\delta(\omega+\mathbf{q}'\cdot\mathbf{v}). \quad (42)$$

By means of (10) and (12) and using $\alpha = 1$ we get

$$\bar{f}(r) = \frac{\sqrt{2}}{(2\pi)^2}\frac{\Gamma(1/4)}{\Gamma(3/4)} h\sigma_0^2 r^{-1/2} \int_0^{+\infty}\mathrm{d}\omega\int_{\omega/v}^{+\infty}\mathrm{d}q\; q^{-1/2} \times J_0(qr)\left(q^2v^2-\omega^2\right)^{-1/2}\mathrm{Im}\,\frac{\omega}{E(\omega,T_q)}. \quad (43)$$

To obtain T_q we need to calculate the Fourier transform of $\bar{f}(r)$:

$$\bar{f}(\mathbf{p}) = \frac{1}{(2\pi)^2}\int \mathrm{d}^2x\;\bar{f}(r)e^{-i\mathbf{p}\cdot\mathbf{x}} = \frac{1}{2\pi}\int \mathrm{d}r\;\bar{f}(r)rJ_0(pr). \quad (44)$$

Substituting (43) into (44) gives

$$\bar{f}(\mathbf{p}) = \frac{1}{4\pi^3}h\sigma_0^2\int_0^{\infty}\mathrm{d}\omega\int_{\omega/v}^{\infty}\mathrm{d}q'q'^{-1/2} \times \mathrm{Im}\left[\frac{\omega}{E(\omega,T_{q'})}\right]\left(q'^2v^2-\omega^2\right)^{-1/2} H(p,q'), \quad (45)$$

where we have used the Weber-Schafheitlin integral formula

$$\int_0^{\infty}\mathrm{d}r r^{1/2}J_0(q'r)\,J_0(pr) = \sqrt{2}\frac{\Gamma(3/4)}{\Gamma(1/4)}H(p,q') \quad (46)$$

with

$$H(p,q) = \begin{cases} p^{-3/2}\left[{}_2F_1\left(3/4,3/4;1;q^2/p^2\right)\right], & q<p, \\ q^{-3/2}\left[{}_2F_1\left(3/4,3/4;1;p^2/q^2\right)\right], & p<q. \end{cases} \quad (47)$$

In (47) the function ${}_2F_1$ is the Gauss hypergeometric function. Substituting (45) and (36) in (35) gives

$$T_q = T_0 + \frac{1}{(2\pi)^2}\frac{2h\sigma_0^2}{\rho C_V}\int_0^{\omega_c}\mathrm{d}\omega\int_{\omega/v}^{q_c}\mathrm{d}q'q'^{-1/2} \times \mathrm{Im}\left[\frac{\omega}{E(\omega,T_{q'})}\right]\left(q'^2v^2-\omega^2\right)^{-1/2} \times \int_0^{q_c}\mathrm{d}p\frac{J_0(p/q)\,H(p,q')}{\left(v^2+D^2p^2\right)^{1/2}}. \quad (48)$$

Equation (48) can be rearranged to give

$$T_y = T_0 + \frac{1}{\pi}\frac{4\gamma_0}{\rho a_0 C_V}\int_0^1\mathrm{d}x x\int_x^1\mathrm{d}z z^{-1/2} \times \mathrm{Im}\left[\frac{E_0}{E(\omega_c x,T_z)}\right]\left(z^2-x^2\right)^{-1/2} \times \int_0^1\mathrm{d}w\frac{J_0(w/y)\,H(w,z)}{\left(1+\xi^2w^2\right)^{1/2}}, \quad (49)$$

where we have used that $h\sigma_0^2 = 4E_0\gamma_{\mathrm{eff}}$ and $a_0\gamma_{\mathrm{eff}} = a\gamma_0$. Here

$$\xi = \xi_0\frac{a_0v_0}{av}, \quad (50)$$

where the dimensionless diffusivity $\xi_0 = 2\pi D/(a_0v_0)$, and where v_0 is a reference velocity. We will assume that the WLF transform is valid so that $E(\omega,T) = E(\omega a_T)$, where

$$a_T = \exp\left[\frac{-8.86(T-T_{\mathrm{g}}-50)}{51.5+T-T_{\mathrm{g}}}\right]. \quad (51)$$

In the calculations presented below we use $T_{\mathrm{g}} = -30\,^{\circ}\mathrm{C}$ for the glass transition temperature.

The set of equations (26, 47, 49, 50), and (51), allows us to calculate the temperature distribution in the rubber, the radius of the crack tip and the energy per unit area needed to propagate the crack.

6 Numerical results: Kelvin model

In what follows we will assume that the rubber obeys the very simple Kelvin rheological model. This is not a very good constitutive model for rubber as it assumes that the material is characterized by a single relaxation time. In reality rubber-like materials have a very wide distribution of relaxation times. However, this should not affect the basic physics and the qualitative picture we present below.

In the Kelvin model the complex elastic modulus of the rubber is given by

$$\frac{1}{E(\omega)} = \frac{1}{E_\infty} + \left(\frac{1}{E_0} - \frac{1}{E_\infty}\right)\frac{1}{1-i\omega\tau}\,, \qquad (52)$$

where typically $E_\infty/E_0 \approx 1000$ or more. Equation (52) gives

$$\mathrm{Im}\left[\frac{E_0}{E(\omega_c x, T_z)}\right] = \kappa\,\mathrm{Im}\left[\frac{1}{1-i\lambda x a_z}\right] = \kappa\frac{\lambda x a_z}{1+\lambda^2 x^2 a_z^2}\,, \qquad (53)$$

where we have introduced the quantities

$$\kappa = 1 - \frac{E_0}{E_\infty}; \qquad \lambda = \omega_c\tau = \frac{v}{v_0}\frac{a_0}{a} \qquad (54)$$

and where a_z stands for a_T for $T = T_q$ with $q = zq_c$. The reference velocity is $v_0 = a_0/(2\pi\tau)$. Substituting (53) in (26) and (49) we get

$$\left(\frac{\gamma_{\rm eff}}{\gamma_0}\right)^{-1} = \left(\frac{a}{a_0}\right)^{-1} = 1 - \kappa\int_0^1 \mathrm{d}y \frac{\lambda a_y}{1+(\lambda y a_y)^2 + \sqrt{1+(\lambda y a_y)^2}} \qquad (55)$$

and

$$T_y = T_0\left[1 + 2\Lambda\kappa\int_0^1 \mathrm{d}z \frac{\lambda a_z}{1+(\lambda z a_z)^2+\sqrt{1+(\lambda z a_z)^2}} \times \int_0^1 \mathrm{d}w \frac{J_0(w/y)\,\hat{H}(z/w)}{(1+\xi^2 w^2)^{1/2}}\right], \qquad (56)$$

where

$$\hat{H}(x) = \begin{cases} x^{3/2}\left[{}_2F_1\left(3/4,3/4;1;x^2\right)\right], & x<1\,,\\ {}_2F_1\left(3/4,3/4;1;1/x^2\right), & x>1\,. \end{cases} \qquad (57)$$

By studying the asymptotic behavior of ${}_2F_1(3/4,3/4;1;x)$ for $x\to 1$, and using that ${}_2F_1(3/4,3/4;1;0) = 1$, a very good interpolation formula has been obtained over the whole range $0 \le x < 1$:

$${}_2F_1(3/4,3/4;1;x) \approx 1 + \frac{2}{\pi}K\left(\frac{1}{2}\right)\left[(1-x)^{-1/2}-1\right] \approx 1 + 1.1803\left[(1-x)^{-1/2}-1\right], \qquad (58)$$

where $K(x)$ is the elliptic integral of the first kind. The dimensionless parameter

$$\Lambda = \frac{\gamma_0}{\rho a_0 C_V T_0}\,. \qquad (59)$$

Within the Kelvin model, $\gamma_{\rm eff}/\gamma_0$ as a function of v/v_0 depends only on the parameters Λ, E_∞/E_0, $T_0 - T_{\rm g}$ and ξ_0. In all numerical calculations presented in this paper we have used $E_\infty/E_0 = 1000$, $T_0 - T_{\rm g} = 50\,\mathrm{K}$, $\Lambda = 10$ or 100, and several values for ξ_0. Since typically $\gamma_0 = 30\ \mathrm{J/m^2}$, $a_0 = 10^{-9}\,\mathrm{m}$, $\rho = 1.2\times 10^3\ \mathrm{kg/m^3}$, $C_V = 1.4\times 10^3\ \mathrm{J/(kg\ K)}$ and $T_0 = 20\,^\circ\mathrm{C}$ we get from (59), $\Lambda \approx 60$.

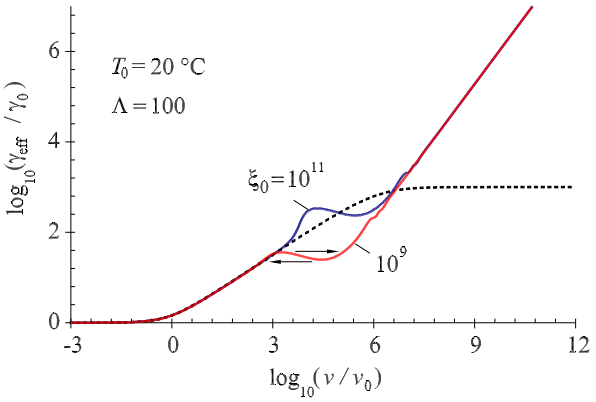

Fig. 4. The effective energy $\gamma_{\rm eff}$ to propagate the crack as a function of the crack velocity v for two different values of the dimensionless diffusivity ξ_0. The dashed line is obtained by neglecting the flash temperature effect. The Kelvin rheological model has been used in the calculation with $E_\infty/E_0 = 1000$ and $\Lambda = 100$. The non-monotonic behavior of the $\gamma_{\rm eff}$ may result in crack motion instability, *e.g.* stick slip motion, as indicated by the black arrows in the picture.

Figure 4 shows the effective energy $\gamma_{\rm eff}$ to propagate the crack as a function of the crack propagation speed for $\Lambda = 100$ and for two different values of $\xi_0 = 2\pi D/(a_0 v_0) = 2\pi D\tau/a_0^2$, corresponding to, *e.g.*, different values of the rubber relaxation time τ. Also shown is the isothermal solution ($T \equiv T_0$; dashed line). At low crack tip velocities the influence of the flash temperature is negligible and all three curves overlap. At higher crack velocities the effective energy $\gamma_{\rm eff}$ required to propagate the crack is non-monotonic, exhibiting a local maximum and a local minimum, which may give rise to crack propagation instabilities. As the velocity is increased further, $\gamma_{\rm eff}$ finally increases proportional to the crack speed.

Figure 5 shows the effective energy $\gamma_{\rm eff}$ to propagate the crack as a function of the crack propagation speed for $\Lambda = 10$ and for different values of ξ_0. Three different regimes are shown: i) the *low-speed* regime, where the increase of temperature in the rubber is negligible; ii) the *hot-crack* regime; and iii) the *cold-crack* regime. The cold-crack regime prevails not only under isothermal condition (corresponding to the heat diffusivity $D = \infty$ or, equivalently $\xi_0 = \infty$), but when D is above some critical value, which in the present case corresponds to $\xi_0 \approx 10^{18}$, the hot-crack regime is absent and crack propagation will follow the cold-crack $\gamma_{\rm eff}(v)$ branch.

Figure 5 shows that for small enough crack velocities (say $v/v_0 < 10^3$) the increase of temperature due to viscous dissipation is negligible and the curves cannot be distinguished from the isothermal curve. Thus, in the low-speed region all curves obey the scaling law $\gamma_{\rm eff}/\gamma_0 \approx (v/v_0)^{0.5}$. For $v/v_0 < 10^{-1}$, $\gamma_{\rm eff}$ is very close to γ_0, and we can smoothly interpolate between these two

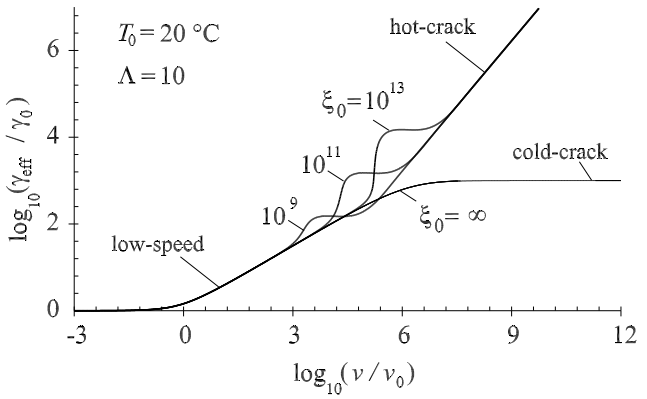

Fig. 5. The effective energy $\gamma_{\rm eff}$ to propagate the crack as a function of the crack velocity v for different values of the dimensionless diffusivity ξ_0. The Kelvin rheological model has been used in the calculations with $E_\infty/E_0 = 1000$ and $\Lambda = 10$. In the transition region between the "low-speed" and the "hot-crack" regimes the effective energy $\gamma_{\rm eff}$ is non-monotonic which may produce crack motion instabilities. In the "low-speed" regime $\gamma_{\rm eff} \sim v^{0.5}$, whereas in the "hot-crack" regime $\gamma_{\rm eff} \sim v$.

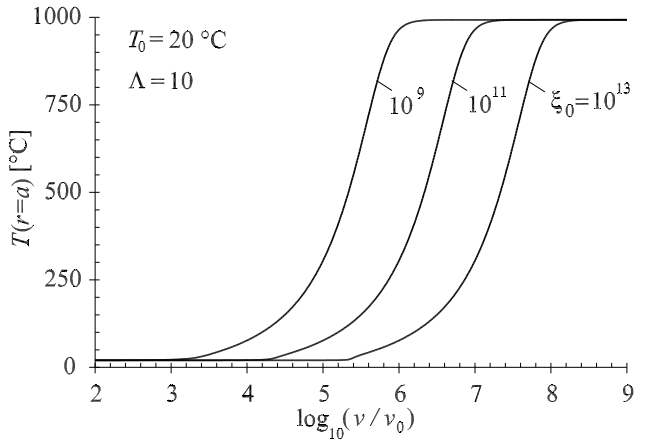

Fig. 6. The crack tip temperature $T(r = a)$ as a function of the crack velocity v. At "low-speed" the temperature rise is negligible. In the transition region the crack tip temperature increases rapidly and becomes constant (and independent of ξ_0) in the "hot-crack" regime.

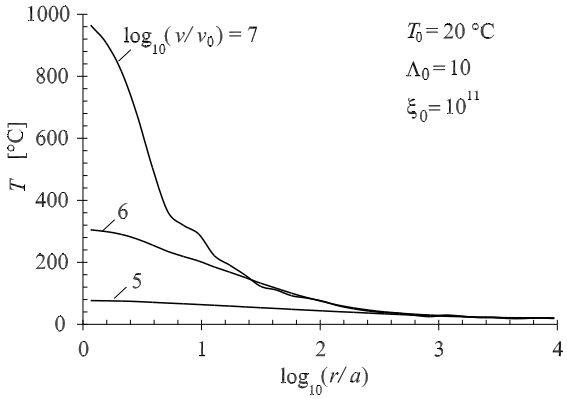

Fig. 7. The temperature profile in front of the crack tip for $\xi_0 = 10^{11}$ and for three different values of crack tip velocity. The temperature increase is significant for $r \lesssim 100a$.

limits using [14]

$$\gamma_{\rm eff} \approx \gamma_0 \left[1 + \left(\frac{v}{v_0}\right)^{0.5}\right]. \tag{60}$$

The exponent of 0.5 is in substantial agreement with the experimental value 0.6 obtained by Maugis and Barquins [5] for polyurethane strips on glass, and also with other theoretical calculations [11, 26]. However, the exact value of the exponent depends on the rubber properties, which are not accurately described by the Kelvin model. Thus, for example, for the styrene-butadiene copolymer rubber [6] the exponent is close to 0.28 [14]. Note also that for the isothermal case the quantity $\gamma_{\rm eff}/\gamma_0 = a/a_0$ goes asymptotically to E_∞/E_0 for very high crack tip velocities (as expected, see App. C). Moreover, in this case we can rewrite (55) as

$$2\kappa\frac{v_0}{v}\left(\frac{\gamma_{\rm eff}}{\gamma_0}\right)^3 + \left(1 - 2\kappa\frac{v_0}{v} - \kappa^2\right)\left(\frac{\gamma_{\rm eff}}{\gamma_0}\right)^2 - 2\left(\frac{\gamma_{\rm eff}}{\gamma_0}\right) + 1 = 0\,, \tag{61}$$

which is an algebraic equation of the third order that can be solved analytically.

At high enough crack speed the temperature rise due to the viscoelastic energy dissipation cannot be neglected. The increase of temperature in front of the crack tip will modify the rheological properties of the rubber, and cause the crack propagation energy to change. Figure 5 shows that for practical applications, where ξ_0 rarely exceeds 10^{13}, the system undergoes a transition from the low-speed regime to the hot-crack regime: first the energy required to propagate the crack rapidly increases, then reaches a local maximum, after which it slightly decreases and then enters the hot-crack region. In the hot-crack region the $\log\gamma_{\rm eff} - \log v$ curve is a straight line with slope equal to 1. This means that the deformation frequency at the crack tip ($\omega = \omega_c = 2\pi v/a$) no longer changes. Also the temperature at the crack tip $T(r = a)$ (see Fig. 6) increases rapidly in the transition region, and then reaches a constant value in the hot-crack region independent of the parameter ξ_0. In fact, for very large crack tip velocities the temperature distribution, as a function of r/a, is velocity independent (see Fig. 7). In the hot-crack regime the frequencies of the pulsating deformations at the crack tip lie in the transition region between the rubbery and the glassy regions of the viscoelastic rubber spectra. In Figure 7 we show the temperature profile in the rubber, as a function of the distance from the crack tip in units of a, for different crack velocities. Notice that for large crack tip velocities the distance region in front of the crack tip where $T \gg T_0$ is quite large, of order $\sim 10a$. Because of the non-uniform temperature distribution, in this large volume element the perturbing frequency v/r will be in

the transition region of the rubber viscoelastic spectra, and a large viscous energy dissipation will occur.

7 Numerical results: Realistic viscoelastic modulus

The complex frequency-dependent modulus of any linear viscoelastic material can be written as

$$\frac{1}{E(\omega)} = \frac{1}{E_\infty} + \int_0^\infty \mathrm{d}\tau \, \frac{H(\tau)}{1 - i\omega\tau}\,, \tag{62}$$

where the spectral density $H(\tau)$ is a real (positive) function of the relaxation time τ. In many cases $E(\omega)$ is well approximated when the spectral density $H(\tau) = A\tau^{-s}$ for $\tau_1 < \tau < \tau_0$, and zero elsewhere. For rubber compounds used for pressure sensitive adhesives one typically has $\tau_0 \approx 1\,\mathrm{s}$ and $\tau_1 \approx 10^{-6}\,\mathrm{s}$ giving $\tau_0/\tau_1 \approx 10^6$.

In Appendix E we show how it is possible to generalize relations (55) and (56) in order to treat this more general case. Figure 8 shows results for $s = 0.6$ (which corresponds, *e.g.*, to a styrene-butadiene copolymer rubber), $\Lambda = 100$ and for two different values of the parameter $\xi_0 = 2\pi D/(a_0 v_0)$. In this case we have defined the reference velocity $v_0 = a_0/(2\pi\tau_1)$, which typically is in the range $v_0 \approx 10^{-2}$–$10^0\,\mathrm{m/s}$. For relative small crack velocities, $\log(\gamma_{\mathrm{eff}}/\gamma_0)$ as a function of $\log(v/v_0)$ is almost a straight line with slope $\simeq 0.28$, in good agreement with the experimental value obtained in reference [6] for the styrene-butadiene rubber, and also in reference [14]. However, when the crack speed is increased above $v \sim 0.01 v_0$, the shape of the curve changes and a non-monotonic behavior is observed which may give rise to crack propagation instabilities. When the crack tip velocity is increased further the crack enters the hot-crack regime. Note that the flash temperature effect becomes important for crack propagation velocities $v > 1\,\mathrm{cm/s}$ in accordance with the qualitative discussion in Section 2. We conclude that, independent of the rubber viscoelastic model under consideration, the flash temperature will always change the shape of the $\log(\gamma_{\mathrm{eff}}/\gamma_0)$ curve in such a way that crack instabilities may be observed. Moreover, for higher crack speed the energy required to propagate the crack increases linearly with the crack speed, and the temperature distribution does no longer change when plotted as a function of r/a. This means that at the crack tip the temperature is also constant. However, the temperature rise at the crack tip may be so high that thermal degradation of the rubber occurs close to the crack tip. This effect was neglected in the theory presented above. When thermal degradation is taken into account (see next section), the maximal crack tip temperature is reduced to more realistic values.

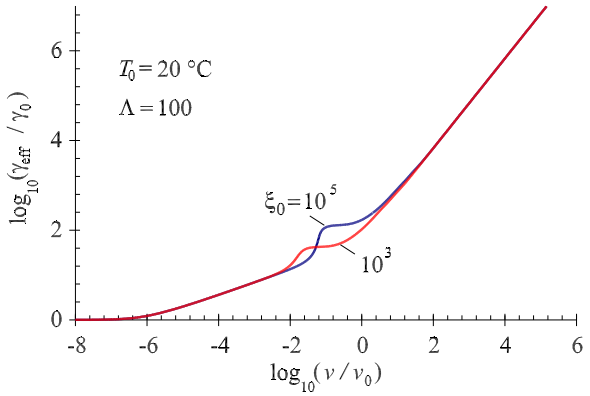

Fig. 8. The effective energy γ_{eff} when the spectral density is $H(\tau) = A\tau^{-s}$ with $s = 0.6$. The frequency of the maximum of the loss tangent of the rubber material is $\omega_2 \approx 10^6\,\mathrm{s}^{-1}$, and the range of rubber relaxation times covers an interval of about six decades.

8 Thermal degradation: Stress-aided thermally activated bond-breaking at the crack tip

The viscoelastic properties of rubber is determined by thermally activated processes involving flipping of polymer segments between different positions. The activation barriers separating the different configurations are typically of order $\sim 0.2\,\mathrm{eV}$. These barriers are much smaller than the energy barriers involved in breaking the chemical bonds at the crack tip, which are of order $\Delta E \sim 1\,\mathrm{eV}$ or more. Hence at not too high temperatures, the main temperature dependence of crack propagation comes from the bulk viscoelastic deformations of the rubber in front of the crack tip. However, even if the temperature is not high enough to generate thermal fluctuations which are large enough to break the bonds at the crack tip, thermal effects are still important for the bond-breaking process for the following reason: during crack propagation, at the crack tip the polymer chains are stretched until they break. However, it is not necessary for the applied force to break the bonds alone, but it is enough to stretch the bond somewhat, *i.e.*, to move the system some distance up toward the top of the barrier ΔE; the remaining part of the barrier can be overcome by a (large enough) thermal fluctuation. At high temperature this *stress-aided thermally activated process* will result in a strong reduction in the stress σ_c at the crack tip during (slow) crack propagation.

A simple analysis of the temperature and velocity dependency of bond-breaking process at the crack tip is based on the following rate equation approach. Consider a polymer chain in front of a crack and assume that the crack tip arrive at the chain at time $t = 0$. The tensile stress acting on the chain at time t ($t < 0$) is *proportional* to (see App. F)

$$\sigma(t) \approx \sigma_c \left(\frac{a}{a - vt}\right)^{1/2}, \tag{63}$$

where a is the crack tip radius and v the crack tip velocity. Thus, the chain is stretched already before the crack tip arrives to it, and the chain may break already for $t < 0$. Let $P(t)$ be the probability that the chain is not broken at time t. Thus,

$$\frac{\mathrm{d}P}{\mathrm{d}t} = -w(t)P, \tag{64}$$

where the rate coefficient

$$w(t) = \nu e^{-\beta U(t)}, \tag{65}$$

where $\beta = 1/k_B T$ and where ν is a prefactor typically of order $\nu \approx 10^{14}\,\mathrm{s}^{-1}$, and where the barrier height (note: $t < 0$) (see App. F)

$$U(t) \approx U_0 \left[1 - \left(\frac{\sigma_c}{\sigma_{c0}}\right)^2 \frac{a}{a - vt}\right],$$

where σ_{c0} is the yield stress at zero temperature, and where $U_0 = \Delta E$. The equations above give (see App. F)

$$\left(\frac{\sigma_c}{\sigma_{c0}}\right)^2 = 1 + \frac{k_B T}{\Delta E} \ln\left[\frac{v}{v_1}\frac{a_0}{a}\left(\frac{\sigma_c}{\sigma_{c0}}\right)^2\right], \tag{66}$$

where

$$v_1 = a_0 \nu k_B T / \Delta E\,.$$

Equation (66) is valid as long as $k_B T/\Delta E \ll 1$. The weakest chemical bonds in rubber are usually multi-sulfur crosslinks such as C-S-S-C, for which $\Delta E \approx 1.2\,\mathrm{eV}$. Single sulfur crosslinks have larger ΔE, and the energy to break a C-C bond in a hydrocarbon chain is much larger, of order 4 eV. In a typical case, for a slowly moving crack, $v_1 \approx 100\,\mathrm{m/s}$. Thus, at room temperature with the crack velocity $v = 1\,\mu\mathrm{m/s}$, one finds from (66) (with $\Delta E = 1.2\,\mathrm{eV}$) that $\sigma_c \approx 0.6\sigma_{c0}$.

We have performed calculations using the theory developed in Section 5 but assuming that the rupture stress σ_c depends on the temperature and the crack tip velocity according to (66). Since $\gamma_0 \sim \sigma_c^2$ this implies that

$$\frac{\gamma_0}{\gamma_{00}} = 1 + \frac{k_B T}{\Delta E} \ln\left(\frac{v}{v_1}\frac{a_0}{a}\frac{\gamma_0}{\gamma_{00}}\right), \tag{67}$$

where $\gamma_{00} = \gamma_0(v, 0)$.

In Figure 9 we show how the thermal degradation affects the crack propagation for a rubber obeying the Kelvin rheological model, using the same parameter values as in Section 6 and with $\Delta E = 2\,\mathrm{eV}$. The effective energy γ_{eff} needed to propagate the crack (see Fig. 9(a)) exhibits the same trend as in Figure 4, except that it is slightly smaller. The term γ_0 initially grows with increasing crack velocity because the force necessary to break a bond at the crack tip increases with increasing bond elongation rate. However, when the increase of temperature becomes significant it decreases very fast, and reaches a nearly constant value at high crack speed (see Fig. 9(b)). The latter follows from the fact that the crack tip temperature is nearly constant for large v. When the thermally activated bond-breaking is taken into account, the increase of temperature at the crack edge is much smaller than when this effect is neglected. Thus, the maximal temperature increase in Figure 9(c) is in the range 630–840 °C in good agreement with experimental results [27]. Note that the asymptotic value of crack tip temperature at high velocities depends on the parameter $\xi_0 = 2\pi D/(a_0 v_0) = 2\pi D\tau/a_0^2$, *i.e.* on the rubber relaxation time τ, the low-velocity crack tip radius a_0, and on the rubber thermal diffusivity D.

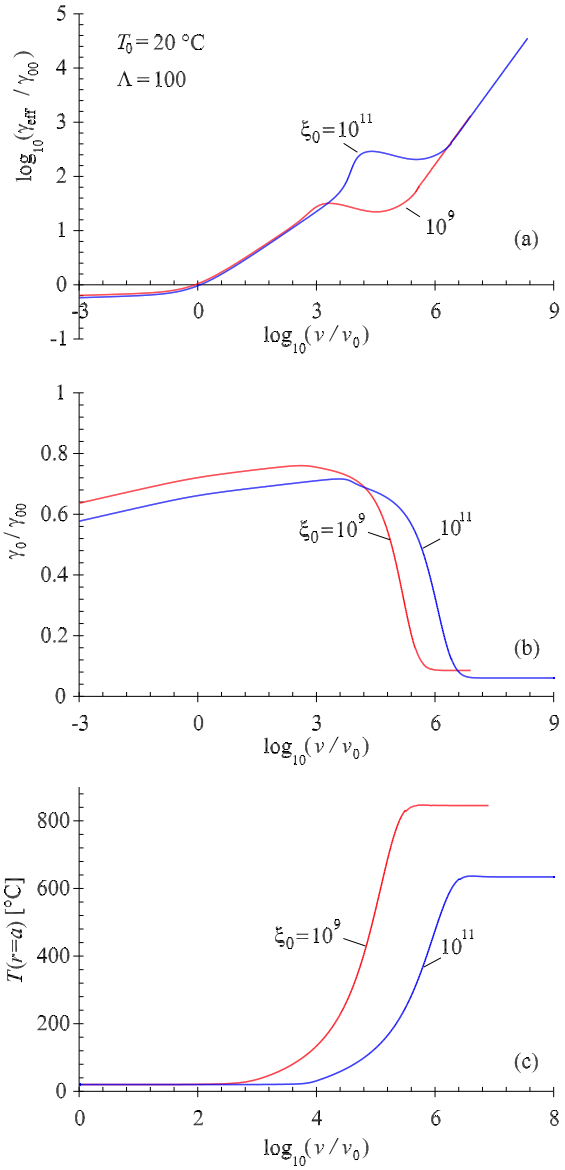

Fig. 9. The influence of the stress-aided thermally activated bond-breaking on crack propagation for a rubber obeying the Kelvin rheological model. (a) The ratio $\gamma_{\mathrm{eff}}/\gamma_{00}$ as a function of the crack propagation velocity (log-log scale). (b) The ratio γ_0/γ_{00} as a function of the crack propagation velocity. Note the fast decrease of γ_0 which occurs when the temperature at the crack tip begins to increase significantly. (c) The crack tip temperature $T(r = a)$ as a function of the crack velocity v. When the thermal degradation effect is considered at the crack tip, the asymptotic value of $T(r = a)$ depends on ξ_0. The maximum temperature is $\lesssim 850\,^\circ\mathrm{C}$, in good agreement with some experiments [27].

9 Discussion

The reason the crack propagation energy increases (for large crack tip velocities) when the crack tip flash temperature effect is taken into account can be understood as follows. Consider a propagating crack and let us first neglect the flash temperature effect, *i.e.*, we assume that

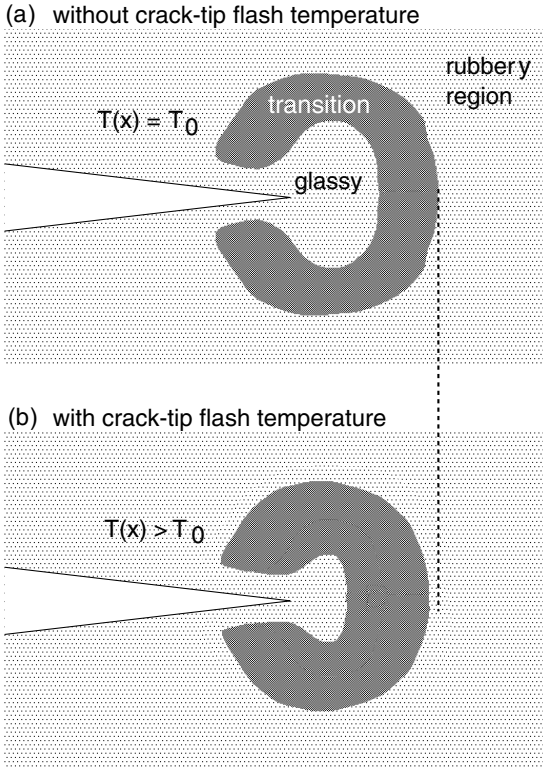

Fig. 10. A qualitative picture of what happens when the flash temperature effect is included in the theory. (a) For isothermal conditions most of the viscoelastic energy dissipation occurs in the transition region between the rubbery and glassy region of the rubber viscoelastic spectra (dark area). (b) When the flash temperature effect is included, because the temperature increase is very large close to the crack tip, the transition region (dark area) extends closer to the crack tip than in (a). On the other hand, the outer rim of the transition region in (a) is converted into the rubbery region. However, since the temperature decreases monotonically with the distance from the crack tip the total energy dissipation increases.

the temperature everywhere equals the background temperature T_0 (Fig. 10(a)). At high crack tip velocity v, the region close to the crack tip is effectively in the glassy state, and contributes very little to the total viscoelastic energy dissipation. Similarly, the region very far away from the crack tip is effectively in the rubbery region of the viscoelastic spectra, and contributes also very little to the total energy dissipation. Most of the viscoelastic energy dissipation occurs in the transition region between the rubbery and glassy region (dark gray area in Fig. 10). Now, let us include the flash temperature effect. Because the crack tip moves toward the region where the viscoelastic energy dissipation occurs, the temperature increase is highest close to the crack tip. Thus, part of what was the glassy region when the temperature effect was neglected will now correspond to the transition region and will contribute strongly to the total viscoelastic energy dissipation. On the other hand, what was the outer rim of the transition region when the flash temperature effect was neglected will now be converted into the rubbery region, and will contribute very little to the total energy dissipation. However, since the temperature decreases monotonically with the distance from the crack tip, the reduction in the energy dissipation in the outer region is overcompensated by the increases in the energy dissipation in the inner region closer to the crack tip. The net effect is that the total energy dissipation *increases* when the flash temperature effect is taken into account. However, a further increase in the velocity increases the temperature even more and shifts the region close to the crack tip toward the rubbery side of the transition region in such a way that $G(v)$ is now nearly constant reaching the flat region of the diagram in Figure 5. However, at very high velocities the region close to the crack tip get shifted back towards the middle of the transition region, and then it stays there for arbitrary high crack tip velocity: when this happens the crack is in the asymptotic *hot-crack* regime. Note, however, that because of heat diffusion, for very low crack tip velocities the temperature increase in the vicinity of the crack tip is negligible, resulting in a negligible increase in the crack propagation energy for small crack tip velocities.

The numerical calculations have shown that beside the *low-speed* and *hot-crack* regimes, at high crack speed another propagation regime can be attained that is what we called the *cold-crack* regime. In this case the temperature increase is almost negligible, and the crack behavior is very close to that one obtained for perfect isothermal conditions. Numerical calculations have shown that the cold-crack regime cannot occur below a certain velocity threshold not depending on ξ_0 provided ξ_0 is not too large. If, instead, ξ_0 is very large, say $\xi_0 > 10^{18}$, as would be the case if the heat diffusivity D of the rubber would be very large, then there is no possibility for the hot-crack regime to occur. In this case, the thermal energy produced by the viscous dissipation diffuses very quickly away from the crack tip region, and since for very high crack tip velocities the energy dissipation occurs in a very large volume very far away from the crack tip, a negligible temperature increase is produced.

The analysis above has only considered the crack propagation energy $G(v)$ for stationary crack propagation (*i.e.*, v constant). However, during stick-slip crack propagation the crack tip velocity is changing in time. This will result in important modifications of the theory, as can be understood by the following qualitative argument. The transitions discussed above involves flipping between the *hot*-crack and the *low-velocity* crack state. In order for the temperature distribution to be fully built up in the hot-crack state the crack must propagate some minimum distance given by the effective radius within which most of the energy dissipation occur in front of the crack tip. For a fast moving crack this distance may be $\sim 100a \sim 1\,\mathrm{mm}$. Similarly, when the system flips from the hot crack state to the low-velocity crack state some time will be needed for the heat produced at the crack tip to diffuse away from the tip region. In a dynamical situation, these effects may result in hysteresis in the transition between the two states as schematically indicated in Figure 11. It implies that the crack propagation energy will not just

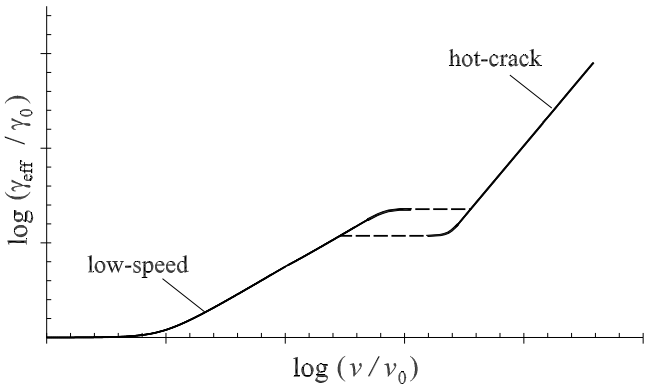

Fig. 11. During stick-slip crack propagation the crack tip velocity is changing in time. This will result in hysteresis in the transition between the *low-speed* regime and the *hot-crack* regime and the crack propagation energy will not just depend on the instantaneous crack tip velocity, but it will depend on the crack tip velocity for all earlier times.

depend on the instantaneous crack tip velocity, but it will depend on the crack tip velocity for all earlier times, *i.e.*, it will be a *functional* of the crack tip position $x(t)$: $G = G(t) = F(x(t'); t' \leq t)$. This situation is analogous to the case of rubber friction, where, because of the flash temperature effect, the rubber friction coefficient is a functional of the sliding history.

Finally, we note that it should be possible to study the temperature rise in the vicinity of the crack tip using an infrared camera with high spatial and temporal resolution.

10 Comparison with experiment

The theory presented above explains why unstable crack propagation is observed in some cases, *e.g.* for tire rubber [16–18]. In ref. [16] two crack propagation modes have been analyzed with two different experimental setups: i) the constrained tension specimen for mode-I loading (Fig. 12(a)), and ii) the trouser specimen for mode-III loading (Fig. 12(b)). Analogous experiments were carried out in reference [17] with the double cantilever beam test. In mode-I loading no stable crack growth is observed, whereas in the trousers test (mode-III loading) stick-slip motion is observed. Here intervals of increase of the load, with no or negligible crack growth, are followed by a sudden decrease of load as the crack propagates fast. We believe that this unstable crack propagation can be explained on the basis of the theory we developed above as follows.

In the transition region between the low-speed regime and the hot-crack regime, a very rapid increase of crack propagation energy is first observed (see Fig. 5), followed by an almost flat region which is smoothly connected to the hot-crack regime. The overall transition region covers a velocity range of about two orders of magnitude. Thus, in a displacement-controlled test, as the system is loaded the crack initially moves very slowly, and when it reaches the transition region its velocity is still very small ($v < 10^{-4}$ m/s) so that its propagation cannot be easily detected. By increasing the displacement further a big amount of energy is stored in the solid, and when the flat area is reached the crack starts to propagate quite fast $v > 10^{-2}$ m/s, giving rise to the observed instability. The reason a stick-slip motion is observed in the trousers test (Fig. 12(b)), whereas a catastrophic failure is observed in mode-I loading (Fig. 12(a)) can be understood as follows.

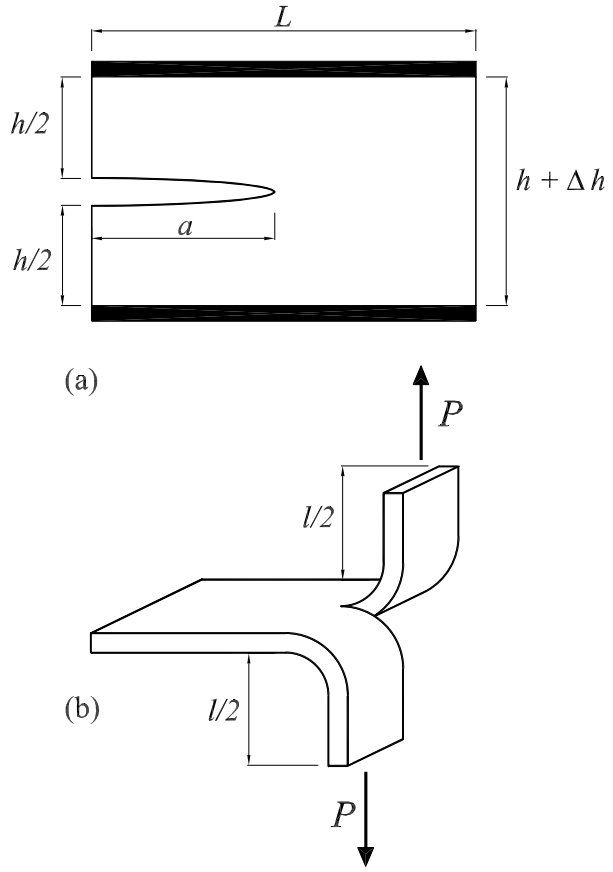

Fig. 12. Two experimental configurations used to study the propagation of cracks in tire rubber. In both cases the experimental tests are performed at controlled displacement: (a) the constrained tension specimen for the mode-I propagation, (b) the trouser specimen setup to analyze the mode-III crack propagation.

In the trousers test, due to the particular constraint conditions, the elastic energy release rate which is available to move the crack decreases very rapidly as the crack propagates. Thus, as soon as the crack begins to grow faster than the speed of separation, the energy release rate will rapidly decrease and the crack will stop. Increasing the displacement increases the energy available to move the crack and allows the cycle to be repeated leading to the observed stick-slip unstable behavior. In the case of mode-I loading (Fig. 12(a)), the elastic energy release rate is constant as the crack propagates. Thus energy is always available to move the crack: once the instability threshold is reached, the crack will propagate fast causing the catastrophic failure of the specimen.

The most detailed experimental study of stick-slip crack propagation in rubber was presented in

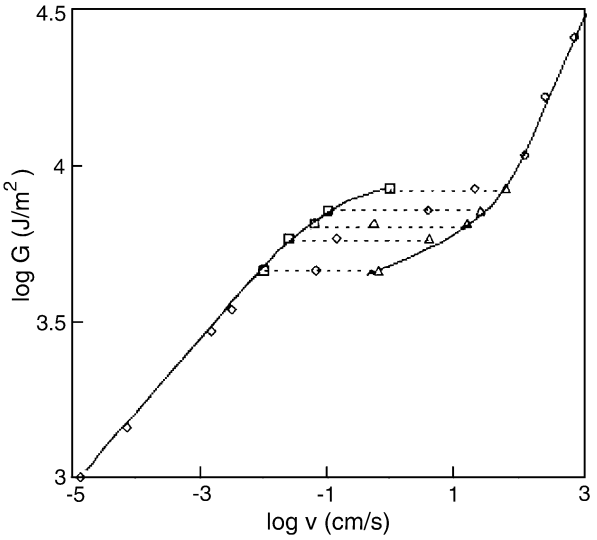

Fig. 13. The crack propagation energy as a function of the crack speed for a styrene-butadiene copolymer rubber with carbon-black filler. The characteristic stick-slip region, where the crack velocity is oscillating in time, is shown as dotted lines (adapted from Ref. [18]).

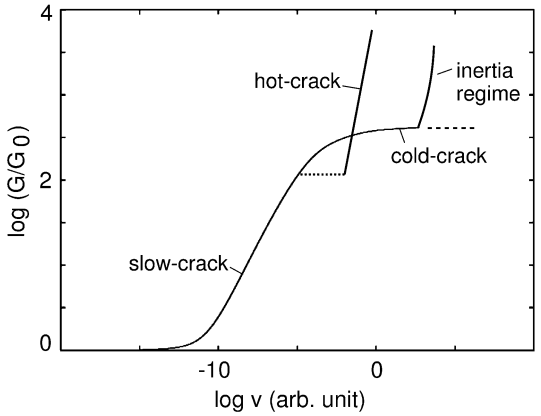

Fig. 14. The relation between the crack propagation energy and the crack tip velocity when inertia effects are included (qualitative diagram). If the crack tip velocity is increased very slowly, the crack will follow the hot-crack branch. However, if the crack tip is initially accelerating very fast, there is not enough time for the full temperature distribution to develop, and the system may follow the cold-crack branch. In the latter case, when the crack velocity becomes of order the sound velocity c, the crack propagation energy will rapidly increase (inertia regime).

reference [18]. In Figure 13 we show the logarithm of the crack propagation energy $G = 2\gamma_{\rm eff}$ as a function of the logarithm of the crack tip velocity for a styrene-butadiene copolymer rubber with carbon black filler. When the (average) crack tip velocity is in the range ~ 0.1–$10\,{\rm cm/s}$ unstable crack propagation occurs. In this velocity region cracks grow at a slow or fast rate corresponding to the data symbols on the left (low-velocity) and right (high-velocity) branch of the $G(v)$ curve in Figure 13. Note also that the slope of the log$G$-log$v$ curve is much higher for the high-velocity branch. Both these facts are in good qualitative agreement with our analytical results (see Figs. 4 and 8). In reference [18] it was also found that the crack surfaces during slow crack propagation (left branch in Fig. 13) was very rough, while very smooth crack surfaces resulted when the crack propagated fast (right branch in Fig. 13). However, this change in surface morphology is not the primary reason for the two $G(v)$ crack propagation branches, but rather a consequence of it. The fundamental reason is instead the flash temperature, and its influence on the viscoelastic energy dissipation in front of the crack tip. We believe that at high crack tip velocities, the high temperature at the crack tip will result in a "liquid-like" region at the crack tip. This in turn will results in the formation of thin uniform layers of modified (degraded) rubber on the crack surfaces. It is clear that information about the peak temperature development during fracture of rubber-like materials can be gained by observing the amount of decomposition products formed by the propagation of the crack [28].

11 Fast cracks in rubber – role of inertia

Recent experiments [29] have detected fast crack propagation in rubber, where the crack tip velocity $\sim 60\,{\rm m/s}$ is of order the rubber sound velocity. We believe that this motion is on the continuation of the cold-crack branch to higher velocities than considered in our study. When the crack velocity becomes of order the sound velocity, inertia effects can no longer be neglected, and the analysis presented above is no longer valid. Nevertheless, from theory [30] one expects the crack propagation energy to rapidly increase as the crack tip velocity approaches the sound velocity c, and we therefore expect the complete relation between the crack propagation energy and the crack tip velocity to take the schematic form indicated in Figure 14.

Slowly moving cracks in rubber have the typical shape shown in Appendix F (see Fig. 17). However, cracks which travel faster than the shear wave speed have wedge-like shape resembling a shock, and recently Marder [31] has developed a shock-wave theory for rapid crack propagation in rubber. The analysis of Marder was based on the elastic free energy density due to Mooney and Rivin. This model account for the non-linear properties of rubber but does not take into account correctly the viscoelastic nature of real rubber-like materials. Thus, the model study of Marder does not account for the increase of the elastic modulus by perhaps a factor of ~ 1000 which will occur close to the crack tip during the fast crack propagation, and it is not clear to us how well the study of Marder is able to describe the fast crack propagation in real rubber.

An important problem is to determine under what circumstances crack propagation will follow the hot-crack branch and the cold-crack branch. If the crack tip velocity is increased very slowly so that the temperature field around the crack tip can be fully developed, our calculations show (see also App. G) that for all physically reasonable rubber parameters, the crack will always follow

the hot-crack branch. However, if the crack tip is initially accelerating very fast, there is not enough time for the full temperature distribution to develop, and in this case the system may follow the cold-crack branch. Thus, we believe that the path the system takes depends on how the crack is generated initially. For example, if a balloon is picked, the resulting crack will accelerate, and in an extremely short time reach a velocity of order the sound velocity, and the system will follow the cold-crack branch. On the other hand, if in trouser tests the legs are pulled with a slowly increasing velocity, the temperature field will at any moment in time be fully developed, and the system will follow the hot-crack branch of the $G(v)$-relation. We believe that this is the explanation why in reference [29] very fast crack propagation was observed when a stretched rubber sheet was picked, while the hot-crack branched was observed in the trouser tests presented in reference [18].

The scenario described above is very similar to the ductile-brittle transition often observed for metals. In some specific temperature regime, if a metal block with a crack is elongated slowly, the metal in the vicinity of the crack edges will undergo very large plastic deformation resulting in a large crack tip radius (blunted tip), and very slow crack growth; in this case the crack propagation energy will be very high because of the large energy involved in the plastic deformation. This crack propagation mode is similar to our hot-crack mode, where a lot of energy is dissipated in front of the crack tip, but now because of viscoelastic deformations rather than plastic deformations. On the other hand, if the elongation is very fast (fast loading) the crack may propagate very fast in a brittle-like manner, involving very small plastic deformation and a much lower crack propagation energy $G(v)$. This is similar to our cold-crack branch.

To summarize, the theory presented in this paper assumes that the crack tip velocity is much smaller than the sound velocity c in rubber. Since typically $c > 10\,\mathrm{m/s}$ this is a good approximation as long as the crack tip velocity is not higher than a few meters per second. At higher crack tip velocities inertia effects become important, and the full $G(v)$-relation is expected to take the qualitative form discussed above.

12 Comments on the crack tip process zone

Classical fracture mechanics, which is based on continuum mechanics, predicts a stress singularity at a crack tip, $\sigma \sim r^{-1/2}$, where r is the distance from the crack tip. However, any real material will yield when the stress becomes high enough. In an ideal brittle material such as mica, the relation $\sigma \sim r^{-1/2}$ may hold until $r \sim a$ is of order a lattice constant a. However, in most materials the $\sigma \sim r^{-1/2}$ relation will break down at a much larger distance r. The spatial region in the vicinity of a crack tip, where the relation $\sigma \sim r^{-1/2}$ is no longer valid is called the *crack tip process zone*.

The crack propagation energy $G = 2\gamma_{\mathrm{eff}}$ will, in general, depend on the exact nature of the processes occurring in the crack tip process zone [32]. Since these bond-breaking processes may be highly complex, *e.g.*, involving cavity formation and stringing, the crack propagation energy in general cannot be calculated accurately but must be deduced from experimental data.

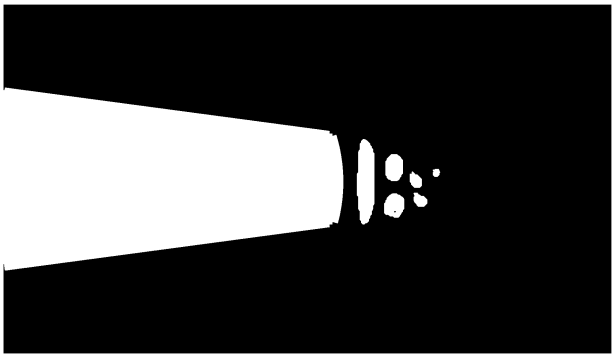

Fig. 15. The crack tip process zone is very complex involving, *e.g.*, cavitation, stringing, chain pull-out (for polymers), and bond-breaking.

The standard model used to describe the crack tip process zone is the Dugdale [33]-Barenblatt [15] model. In this model it is assumed that the bond-breaking at the crack tip occurs by stretching the bonds orthogonal to the crack surfaces until they break at some characteristic stress level σ_c. The process zone extends a distance a in front of the crack tip. This model was first applied to crack propagation in viscoelastic solids by Schapery [10], and later by Greenwood and Johnson [11], Barber *et al.* [12], and by Hui *et al.* [13]. A different approach based on energy balance was used by Christensen [22, 23], and a very simple treatment was presented by Persson and Brener [14]. All these studies neglected the temperature increase at the crack tip due to the viscoelastic energy dissipation. Under the hypothesis of isothermal crack propagation, these models gave results which agree with those obtained in the present paper and in reference [14]. In particular, it has been shown that during crack growth γ_{eff} may increase by a factor of $\sim 10^3$, or more, as the crack tip velocity increases. It is also important to notice that during crack closure γ_{eff} is instead smaller than γ_0 [14]. This large hysteresis in the adhesion energy, γ_{eff}, during crack growth and closure, has also been observed experimentally [34], and may give an important contribution to the friction force during sliding of a rubber block on a smooth asperity, as the sliding process can be considered as resulting from a closing crack at the front edge of the contact region, and an opening crack at the trailing edge [3].

Following reference [14], the present treatment introduces the cut-off length in a more *ad hoc* manner than in most earlier treatments, which may be roughly interpreted as a blunting of the crack tip. This approach results in much simpler equations than those obtained within the Barenblatt model of the crack tip process zone. Furthermore, with some additional mathematical effort, it can (approximately) account for the flash temperature effect due to the viscoelastic energy dissipation in the solid. The exact way the cut-off is introduced is unimportant [14], and different models give almost the same results [11, 12].

In reality, the process zone is much more complex than assumed in the theory, see Figure 15. Thus, the cut-off should be introduced in such a way as to simplify the analytical calculations as much as possible, and for crack propagation in viscoelastic solids we believe that our cut-off procedure results in the simplest formalism. Only the factor G_0 in equation (1) depends on the crack tip process zone, but for polymers this quantity cannot be calculated accurately at present. However, in the present paper we have presented a simple model for G_0 which can be used to estimate the velocity and temperature dependence of G_0 for high temperatures.

When the flash temperature effect is negligible the present theory agrees substantially with other theoretical studies and with experiment. However, compared to other theories the formalism used is much simpler and, as shown above, this makes it possible to account for the flash temperature effect. The present theory predicts the influence of the flash temperature on the crack propagation behavior, and it shows that the flash temperature may result in unstable crack propagation, *e.g.* stick-slip motion or catastrophic failure.

13 Conclusion

In this paper we have studied crack propagation in viscoelastic solids. We have calculated the dependence of the fracture energy (per unit area) $G = 2\gamma_{\rm eff}$ on the crack velocity v including the effect of the flash temperature. Because of the low heat conductivity of rubber materials, the crack tip flash temperature is extremely important already at relative low crack tip velocities. The theory explains why unstable crack propagation is observed in many experiments. The flash temperature modifies the function $\gamma_{\rm eff}(v)$ in such a way that it becomes non-monotonic. Thus, depending on the crack speed, unstable crack motion may occur, *e.g.* stick-slip motion or catastrophic failure.

We note that it should be possible to study the temperature rise in the vicinity of the crack tip using a high-resolution infrared camera.

In isothermal conditions, when the temperature is equal to the background temperature everywhere in the rubber, the present theory gives results similar to those based on the Dugdale-Barenblatt model in spite of the very different treatment of the crack tip process zone. This shows that the exact nature or shape of the crack tip process zone is not important for the velocity dependence of $G(v)$, as long as the size $a(v)$ of the process zone increases with increasing crack tip velocity v in such a way that the stress at the crack tip does not exceed the critical value σ_c for bond-breaking.

In many applications the external driving stress is not constant but is oscillating in time. This may result in slow crack propagation even when the amplitude of the stress is very small, sometimes causing fatigue failure. We think that the temperature increase at the crack tip should significantly affect the crack propagation under fatigue test conditions, as already observed in some experiments [35]. We are at present studying this effect and will report on the results elsewhere.

Appendix A. Energy dissipation per unit time in a linear viscoelastic material

Consider first a viscoelastic solid subjected to a stress field $\sigma_{ij}(\mathbf{x}-\mathbf{v}t)$ propagating with velocity $\mathbf{v}$ in the solid. Suppose that $\sigma_{ij}(\mathbf{x})$ is square integrable, so that $\sigma_{ij}(\mathbf{x}) \to 0$ as $|\mathbf{x}| \to +\infty$. In this case the total elastic energy stored in the solid does not vary with time, and the work per unit time done by the internal stresses is just the energy dissipation per unit time

$$P = \int {\rm d}^3x\ \dot{\varepsilon}_{ij}\sigma_{ij}\,. \tag{A.1}$$

Under the given hypotheses the stress field may be represented by means of its Fourier transforms as

$$\sigma_{ij}(\mathbf{x}) = \int {\rm d}^2q\ \sigma_{ij}(\mathbf{q})\, e^{i\mathbf{q}\cdot\mathbf{x}}\,. \tag{A.2}$$

Now in linear viscoelastic materials the time Fourier transform of the strain field is related to the time Fourier transform of the stress field by means of the relation $\sigma_{ij}(\mathbf{x},\omega) = E_{ijkh}(\omega)\,\varepsilon_{kh}(\mathbf{x},\omega)$, where the tensor $E_{ijkh}(\omega)$ is the complex elastic modulus of the material. Thus, we can write

$$\dot{\varepsilon}_{ij}(\mathbf{x},t) = \int {\rm d}\omega\,(-i\omega)\,\varepsilon_{ij}(\mathbf{x},\omega)\,e^{-i\omega t} = \int {\rm d}\omega\,(-i\omega)\,C_{ijkh}(\omega)\,\sigma_{kh}(\mathbf{x},\omega)\,e^{-i\omega t}\,, \tag{A.3}$$

where the tensor $C_{ijkh}(\omega) = [E_{ijkh}(\omega)]^{-1}$. Now observe that

$$\sigma_{ij}(\mathbf{q},t) = \frac{1}{(2\pi)^2}\int {\rm d}^2x\ \sigma_{ij}(\mathbf{x}-\mathbf{v}t)\,e^{-i\mathbf{q}\cdot\mathbf{x}} = e^{-i\mathbf{q}\cdot\mathbf{v}t}\frac{1}{(2\pi)^2}\int {\rm d}^2x\ \sigma_{ij}(\mathbf{x})\,e^{-i\mathbf{q}\cdot\mathbf{x}} e^{-i\mathbf{q}\cdot\mathbf{v}t}\sigma_{ij}(\mathbf{q}) \tag{A.4}$$

and that

$$\sigma_{ij}(\mathbf{x},\omega) = \frac{1}{2\pi}\int {\rm d}t\ \sigma_{ij}(\mathbf{x},t)\,e^{i\omega t} = \int {\rm d}^2q\ \sigma_{ij}(\mathbf{q})\,\delta(\omega-\mathbf{q}\cdot\mathbf{v})\,e^{i\mathbf{q}\cdot\mathbf{x}}\,. \tag{A.5}$$

Therefore we can write $\dot{\varepsilon}_{ij}$ as

$$\dot{\varepsilon}_{ij}(\mathbf{x},t) = \int {\rm d}^2q\ \sigma_{kh}(\mathbf{q})\,(-i\mathbf{q}\cdot\mathbf{v})\,C_{ijkh}(\mathbf{q}\cdot\mathbf{v})\,e^{i\mathbf{q}\cdot(\mathbf{x}-\mathbf{v}t)}. \tag{A.6}$$

Substituting (A.6) in (A.1) gives

$$P = (2\pi)^2\int {\rm d}^2q\,(-i\mathbf{q}\cdot\mathbf{v})\,C_{ijkh}(\mathbf{q}\cdot\mathbf{v})\,\sigma_{ij}(-\mathbf{q})\,\sigma_{kh}(\mathbf{q})\,. \tag{A.7}$$

Appendix B. Stress at the crack tip

In this appendix we explain the origin of the $\sim r^{1/2}$-dependence of the stress field at the crack tip. Neglecting inertia effects, the stress tensor satisfies the equilibrium relation

$$\sigma_{ij,j} = 0\,. \tag{B.1}$$

In addition, the stress tensor must satisfy certain compatibility conditions, which, as long as the relation between the stress and strain is linear, and the material homogeneous and isotropic, are independent of the constitutive relation between the stress and the strain. For the plane stress or strain case which is of interest here (where the stress tensor is independent of z), the compatibility equation becomes

$$\nabla^2(\sigma_{xx} + \sigma_{yy}) = 0\,. \tag{B.2}$$

Note that (B.1) and (B.2) constitute three independent equations for three unknown quantities, namely σ_{xx}, σ_{yy} and σ_{xy}. It follows that the stress distribution in the vicinity of a crack tip has the universal form $\sim r^{-1/2}$ independent of the detailed form of the constitutive relation between stress and strain as long as the relation is linear and the material homogeneous and isotropic, *i.e.*, it is also valid for a viscoelastic solid.

When a non-uniform temperature distribution occurs at the crack tip, the arguments presented above for the $r^{-1/2}$ stress singularity, are not strictly valid. To illustrate that this is not a trivial point let us note that even for a constant temperature, the effective hardness of the rubber will vary with the distance r from the crack tip, perhaps from a hard glassy region close to the crack tip to a very soft rubbery behavior far away, simply as a result of the difference of the perturbing frequencies $\omega \sim v/r$. However, as is proved above, this difference in elastic hardness has *no influence* on the stress singularity $\sim r^{-1/2}$. However, the temperature profile has a different influence on the viscoelastic modulus than that which results from the variation in the perturbing frequencies.

Appendix C. Asymptotic value of the crack propagation energy

Let us prove that, when the temperature in the rubber is constant, during crack opening at very high velocities the following relation is obtained:

$$\lim_{v\to\infty}\gamma_{\rm eff}(v) = \gamma_0 E_\infty/E_0\,. \tag{C.1}$$

This relation is not valid during crack closing. As shown above the stress in the vicinity of the crack tip has the universal form

$$\sigma = K(2\pi r)^{-1/2}\,, \tag{C.2}$$

where the stress intensity factor K is proportional to the external applied stress. Assume that the crack tip propagates with a velocity v. The deformation rate of the viscoelastic solid at a distance r from the crack tip is characterized by the frequency $\omega = v/r$. Now, the smallest possible r is a molecular distance a. Hence, the highest possible frequency will be v/a. For very low velocity this frequency will be in the rubbery region of the viscoelastic spectra $E(\omega)$ and in this case the solid will behave purely elastically everywhere with the elastic modulus $E_0 = E(0)$. In this case no dissipation in the bulk occurs and the crack propagation energy is $G = 2\gamma_0$.

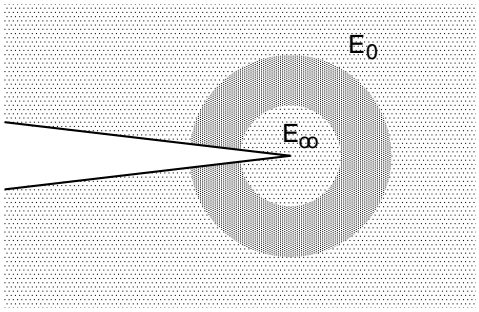

Fig. 16. When a crack propagates fast in viscoelastic solids it is possible to distinguish between three separate regions: a) an inner region where the perturbing frequencies $\omega = v/r$ are in the hard glassy region of the rubber viscoelastic spectra, characterized by the high-frequency elastic modulus E_∞, b) an outer region where the perturbing frequencies correspond to the rubbery region characterized by the zero-frequency modulus E_0, and c) an intermediate region where the full complex viscoelastic modulus $E(\omega)$ enters, and where most of the energy dissipation occurs.

Next consider very high crack velocity v. Thus, for small enough r the frequency ω will be so high that the rubber response will correspond to the glassy region where the elastic modulus is $E(\omega) \approx E_\infty$. On the other hand, when r is large enough the frequency $\omega = v/r$ will correspond to the rubbery region where $E(\omega) \approx E_0$. At intermediate distances $E(\omega)$ is complex and this "dissipative" region is indicated by the dark-gray area in Figure 16. Now, let us consider the crack propagation energy G which for an elastic medium in plane stress conditions is related to the stress intensity factor K via

$$G = K^2/E. \tag{C.3}$$

We first apply this formula to the inner region at the crack tip. In this case $G = G_0 = 2\gamma_0$ and $E = E_\infty$ giving

$$2\gamma_0 = K^2/E_\infty\,. \tag{C.4}$$

When we study the system at a lower magnification we do not observe the inner region and the dissipative region but only the outer region. In this case we must include in the crack propagation energy the energy dissipation in the rubber in the transition region (dark-gray area in Fig. 16). Thus, G will now be larger than $2\gamma_0$ and we write for the outer region $G = 2\gamma_{\rm eff}$. Since $E = E_0$ in the outer region, we get

$$2\gamma_{\rm eff} = K^2/E_0\,. \tag{C.5}$$

Combining (C.4) and (C.5) gives (for $v \to \infty$)

$$\gamma_{\rm eff} = \gamma_0 E_\infty/E_0. \tag{C.6}$$

Appendix D. A sum rule for the viscoelastic modulus E(ω)

Let us prove the sum rule given by equation (21). The viscoelastic modulus $E(\omega)$ and the inverse $1/E(\omega)$ are causal linear response functions. For example, causality implies that the strain $\epsilon(t)$ in a solid at time t only depends on the stress $\sigma(t')$ it was exposed to at earlier times $t' \leq t$, *i.e.*,

$$\epsilon(t) = \int_{-\infty}^{t} \mathrm{d}t' \; C(t-t')\sigma(t') \,. \tag{D.1}$$

Defining the Fourier transform

$$\epsilon(\omega) = \frac{1}{2\pi} \int_{-\infty}^{\infty} \mathrm{d}t \; \epsilon(t) e^{i\omega t} \,, \tag{D.2}$$

we get from (D.1)

$$\epsilon(\omega) = \sigma(\omega)/E(\omega) \,, \tag{D.3}$$

where

$$\frac{1}{E(\omega)} = \int_0^{\infty} \mathrm{d}t \; C(t) e^{i\omega t} \,. \tag{D.4}$$

Since $\mathrm{Re}\,(i\omega t) < 0$ for $t > 0$ and $\mathrm{Im}\,(\omega) > 0$ it follows that $1/E(\omega)$ is an analytical function of ω in the upper half of the complex frequency plane. Thus all poles and branch cuts of $1/E(\omega)$ will occur in the lower part of the complex ω-plane and we may write

$$\frac{1}{E(\omega)} = \frac{1}{E_\infty} + \int_0^{\infty} \mathrm{d}\tau \; \frac{H(\tau)}{1 - i\omega\tau} \,, \tag{D.5}$$

where the *spectral density* $H(\tau)$ is real and positive. Using (D.5) one can easily prove the *sum rule*

$$\frac{1}{E(0)} - \frac{1}{E(\infty)} = \frac{2}{\pi} \int_0^{\infty} \mathrm{d}\omega \; \frac{1}{\omega} \mathrm{Im} \frac{1}{E(\omega)} \,. \tag{D.6}$$

Appendix E. A more general viscoelastic model

The Kelvin viscoelastic model is not a good description of rubber-like materials because it depends on a single relaxation time while rubber-like materials have a wide distribution of relaxation times. A better description of the rubber behavior can be achieved considering a discretized version of the general formula (D.5). We assume that the *spectral density* $H\,(\tau)$ is different from zero only in a finite interval $\tau_1 \leq \tau \leq \tau_0$. In this case, with the substitution $\tau = \tau_1 e^{\mu}$, we have

$$\begin{aligned} \frac{1}{E(\omega)} &= \frac{1}{E_\infty} + \int_0^{\mu_0} \mathrm{d}\mu \; \frac{\tau_1 e^{\mu} H(\tau_1 e^{\mu})}{1 - i\omega\tau_1 e^{\mu}} \\ &\approx \frac{1}{E_\infty} + \tau_1 \Delta\mu \sum_{k=0}^{n-1} \frac{e^{k\Delta\mu} H_k}{1 - i\omega\tau_1 e^{k\Delta\mu}}, \end{aligned} \tag{E.1}$$

where $H_k = H(\tau_1 e^{k\Delta\mu})$, $n\Delta\mu = \mu_0$, and $\mu_0 = \log(\tau_0/\tau_1)$. Putting $\omega = 0$ in (E1) gives

$$\tau_1 \Delta\mu = \frac{1}{\sum_{k=0}^{n-1} e^{k\Delta\mu} H_k} \left(\frac{1}{E_0} - \frac{1}{E_\infty} \right).$$

Thus, (E1) can be written as

$$\frac{E_0}{E(\omega)} = (1-\kappa) + \kappa \frac{1}{\sum_{k=0}^{n} e^{k\Delta\mu} H_k} \sum_{k=0}^{n} \frac{e^{k\Delta\mu} H_k}{1 - i\omega\tau_1 e^{k\Delta\mu}}, \tag{E.2}$$

where $\kappa = 1 - E_0/E_\infty$. If the spectral density $H\,(\tau) = A\tau^{-s}$, we get

$$\frac{E_0}{E(\omega)} = (1-\kappa) + \kappa \frac{1}{\sum_{k=0}^{n} e^{k\Delta\mu(1-s)}} \sum_{k=0}^{n} \frac{e^{k\Delta\mu(1-s)}}{1 - i\omega\tau_1 e^{k\Delta\mu}} \,. \tag{E.3}$$

Using this rheological model in (23) and (49) one obtain the following expressions for the effective adhesion energy γ_{eff}, and the temperature distribution:

$$\begin{aligned} \left(\frac{\gamma_{\mathrm{eff}}}{\gamma_0} \right)^{-1} &= 1 - \frac{\kappa}{\sum_{k=0}^{n} e^{k\Delta\mu(1-s)}} \sum_{k=0}^{n} e^{k\Delta\mu(1-s)} \\ &\times \int_0^1 \mathrm{d}y \frac{\lambda a_y e^{k\Delta\mu}}{1 + (y\lambda a_y e^{k\Delta\mu})^2 + \sqrt{1 + (y\lambda a_y e^{k\Delta\mu})^2}}, \end{aligned} \tag{E.4}$$

$$\begin{aligned} \frac{T_y}{T_0} &= 1 + \frac{2\Lambda\kappa}{\sum_{k=0}^{n} e^{k\Delta\mu(1-s)}} \sum_{k=0}^{n} e^{k\Delta\mu(1-s)} \\ &\times \int_0^1 \mathrm{d}z \frac{\lambda a_z e^{k\Delta\mu}}{1 + (\lambda z a_z e^{k\Delta\mu})^2 + \sqrt{1 + (\lambda z a_z e^{k\Delta\mu})^2}} \\ &\times \int_0^1 \mathrm{d}w \frac{J_0\,(w/y)\,\hat{H}\,(z/w)}{(1 + \xi^2 w^2)^{1/2}}. \end{aligned} \tag{E.5}$$

Here we have $\lambda = \omega_c \tau_1$ and $v_0 = a_0/\,(2\pi\tau_1)$.

Appendix F. Stress-aided thermally activated bond-breaking at the crack tip

We assume the following basic picture for the bond-breaking at the crack tip. To break the strong covalent bonds in the hydrocarbon chains requires very high local stress σ_c^*. The crack tip yield or rupture stress σ_c in the theory presented in this paper is typically of order $\sigma_c \sim 10\,\mathrm{MPa}$, which is many orders of magnitude smaller than the local stress σ_c^* necessary to break the covalent bonds. However, the stress σ_c is so high that the polymer chains have been largely straighten out, and the rubber (because of the non-linear elastic modulus) stiffened to the extent that the rubber in the process zone has become brittle-like. Thus, in the crack tip process zone, strong stress concentration will occur close to any crack-like defect which may result in local bond-breaking. This may

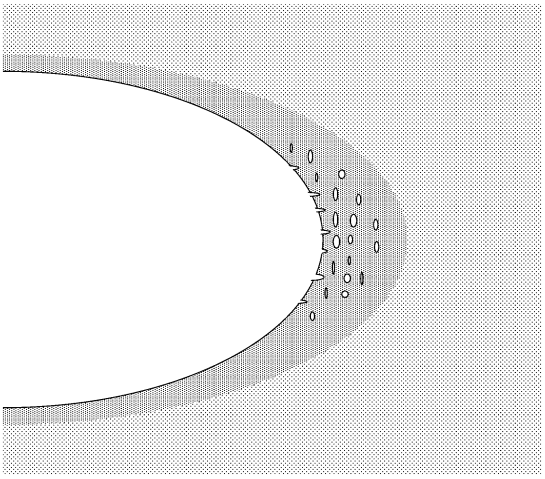

Fig. 17. In the crack tip process zone crack-like defects occur. The average stress in the crack tip process zone is of the order of the rupture stress σ_c but the local stress σ_c^* at the tips of the crack-like defects may be high enough to break the strong chemical bonds in the hydrocarbon chains. We assume that σ_c^* is proportional to the average stress σ_c.

occur simultaneously at many places in the crack tip process zone, resulting in a very inhomogeneous and defect-rich (degraded) rubber which finally fails (see Fig. 17). The following calculations will be based on the assumption that the local stress σ_c^* (at the tip of a crack-like defect) necessary for bond-breaking, is proportional to the yield or rupture stress σ_c.

Consider a polymer chain in front of the crack tip. Let k be the spring constant of a bond in the chain. If a force F elongates the chain, the bond length will increase with $u = F/k$. If ΔE is the energy necessary to break the bond, then we define the critical displacement u_c so that $\Delta E = ku_c^2/2$. If the bond has been elongated by the amount u the barrier which must be overcome by a thermal fluctuation in order to break the bond will be

$$U = \frac{1}{2}k\left(u_c^2 - u^2\right) = \Delta E\left[1 - \left(\frac{u}{u_c}\right)^2\right].$$

Since the displacement $u = F/k$ is proportional to the stress σ, we can also write

$$U = \Delta E\left[1 - \left(\frac{\sigma}{\sigma_{c0}}\right)^2\right], \tag{F.1}$$

where σ_{c0} is the rupture stress at zero temperature. Substituting (63) in this equation gives

$$U = \Delta E\left[1 - \left(\frac{\sigma_c}{\sigma_{c0}}\right)^2 \frac{a}{a - vt}\right]. \tag{F.2}$$

The probability that the bond is not broken at time t (note $t \leq 0$) can be obtained by integrating (64) which gives

$$P(t) = \exp\left(-\int_{-\infty}^{t} \mathrm{d}t'\ w(t')\right), \tag{F.3}$$

where we have used that $P(t) = 1$ for large (negative) times. We can determine the rupture stress σ_c (which depends on the temperature T and the crack tip velocity v) by the requirement that with high probability the bond is broken when the crack tip arrives to the polymer chain (or segment) under consideration. The result for $\sigma_c(v, T)$ is very insensitive to the exact definition, and it is convenient to use the condition $P(0) = 1/e$. Thus, using (F.3) we get

$$P(0) = \exp\left(-\int_{-\infty}^{0} \mathrm{d}t'\ w(t')\right) = 1/e$$

or

$$\int_{-\infty}^{0} \mathrm{d}t\ w(t) = 1. \tag{F.4}$$

Substituting (65) in (F.4) gives

$$\int_{-\infty}^{0} \mathrm{d}t\ \nu \exp\left[-\beta U(t)\right] = 1. \tag{F.5}$$

Substituting (F.2) in (F.5) and changing integration variable to $x = 1 - vt/a$ gives

$$\int_{1}^{\infty} \mathrm{d}x\ \exp\left(-\beta\Delta E\left[1 - \left(\frac{\sigma_c}{\sigma_{c0}}\right)^2 \frac{1}{x}\right]\right) = \frac{v}{\nu a}. \tag{F.6}$$

The integral in this expression diverges. This results from the large x-contribution to the integral. However, this divergence is of no physical significance and just corresponds to the fact that at any finite temperature all bonds break after a long enough time. In fact, for $k_BT/\Delta E \ll 1$ the only important contribution to the x-integral in (F.6) comes from $x \approx 1$ (*i.e.*, from $-vt/a < 1$), and we may replace $x = 1 + \xi$ and expand $1/(1 + \xi) \approx 1 - \xi$ to first order in ξ. This gives

$$\int_{0}^{\infty} \mathrm{d}\xi\ \exp\left(-\beta\Delta E\left[1 - \left(\frac{\sigma_c}{\sigma_{c0}}\right)^2 (1 - \xi)\right]\right) = \frac{v}{\nu a}.$$

Performing the integral gives

$$\exp\left(-\beta\Delta E\left[1 - \left(\frac{\sigma_c}{\sigma_{c0}}\right)^2\right]\right) = \frac{\beta\Delta E v}{\nu a}\left(\frac{\sigma_c}{\sigma_{c0}}\right)^2$$

or

$$\left(\frac{\sigma_c}{\sigma_{c0}}\right)^2 = 1 + \frac{k_BT}{\Delta E}\ln\left[\frac{v}{v_1}\frac{a_0}{a}\left(\frac{\sigma_c}{\sigma_{c0}}\right)^2\right],$$

where

$$v_1 = a_0\nu k_BT/\Delta E.$$

Appendix G. The fully calculated G(v) curve

As already stated in Section 11, here we show that depending on how the crack propagation process is initiated, quite fast cracks may follow either the hot-crack branch or the

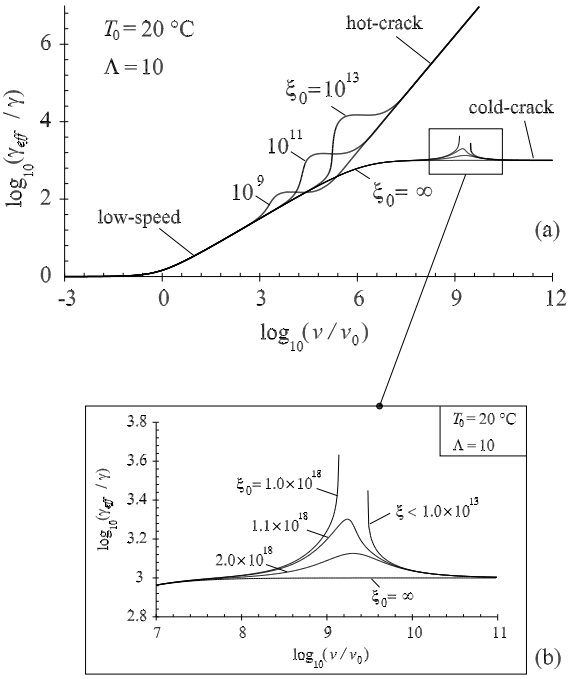

Fig. 18. The effective energy to propagate the crack as a function of the crack propagation speed for different values of ξ_0 (a). Some curves are also plotted for very high values of ($\xi_0 > 10^{18}$), and in the limiting case of isothermal conditions ($\xi_0 \to \infty$) (b). Note that for physically reasonable values of $\xi_0 < 10^{13}$ and quite fast-moving cracks, say $\log_{10}(v/v_0) > 9$, both the cold-crack and the hot-crack regimes are permitted.

cold-crack branch of the $G(v)$ diagram. In fact the numerical calculations have shown that for all physically plausible rubber parameters, the $G(v)$ curve shows a branch point (where the number of solutions changes from one to two), which occurs when the crack velocity exceeds a certain value dependent on the viscoelastic properties of the rubber. Thus, depending on how the crack propagation process evolves, a significant increment of temperature may be produced or not. If the crack tip velocity is increased very slowly (quasi-stationary process) then the crack will always follow the hot-crack branch but if for some reasons the increase of temperature is avoided then the system may follow the cold-crack branch. Our calculations consider a steady-state crack propagation, therefore our theory is not completely able to determine in which conditions fast moving cracks will follow the cold branch, but nevertheless it shows that this may happen because of the occurrence of a branch point into the solution.

Figure 18(a) shows the effective energy γ_{eff} to propagate the crack as a function of the crack propagation speed for different values of $\xi_0 = 2\pi D/(a_0 v_0)$. In this case the linear viscoelastic Kelvin model has been used. Some curves are also plotted for very high values of ξ_0 ($\xi_0 > 10^{18}$), and in the limiting case of isothermal conditions ($\xi_0 \to \infty$) (see inset in Fig. 18(b)). In this case the hot-crack regime is suppressed, *i.e.* the temperature is always very close to the background temperature T_0. Also note that for physically reasonable values of ξ_0 (say $\xi_0 < 10^{13}$) and quite fast-moving cracks, say ($\log_{10}(v/v_0) > 9$), both the cold-crack and the hot-crack regimes are permitted, whereas if $\xi_0 > 10^{18}$, *i.e.* for very high values of the diffusivity D of the rubber, the $G(v)$-function is a single valued function and no branch point occurs. Also observe that the cold-crack regime actually represents an unstable behavior of the system. On the cold-crack curve the energy required to propagate the crack decreases as the crack speed is increased. Thus, a very small reduction of the crack speed would increase the energy required to propagate the crack, this in turn will cause a further reduction of the crack speed until crack arrests. Vice versa, a small increase of the crack velocity would cause a reduction of the crack propagation energy. Therefore in the cold-crack regime, if the energy available to propagate the crack is enough, the crack will accelerate till to reach a new stable point located, this time, on the inertia regime curve (see Fig. 14) with a propagation speed close to the sound velocity.

Numerical calculations have shown that if ξ_0 is very large ($\xi_0 > 10^{18}$), the thermal energy produced by the viscoelastic dissipation diffuses very quickly away from the crack tip region, and since for very high crack tip velocities the energy dissipation occurs in a very large volume very far away from the crack tip, a negligible temperature increase is produced. Thus, as a function of the crack tip velocity, we expect a temperature-induced peak-like structure in the crack propagation energy, as indeed observed in the calculations (see Fig. 18(b)).

References

1. G. Heinrich, J. Stuve, G. Gerber, Polymer **43**, 395 (2002).
2. C. Creton, H. Lakrout, J. Polym. Sci. B, Polym. Phys. **38**, 965 (2000).
3. G. Carbone, L. Mangialardi, J. Mech. Phys. Solids **52**, 1267 (2004).
4. A.N. Gent, J. Schultz, J. Adhes. **3**, 281 (1972).
5. D. Maugis, M. Barquins, J. Phys. D **11**, 1989 (1978).
6. A.N. Gent, Langmuir **12**, 4492 (1996).
7. M.L. Williams, R.F. Landel, J.D. Ferry, J. Am. Chem. Soc. **77**, 3701 (1955).
8. B.N.J. Persson, J. Chem. Phys. **115**, 3840 (2001).
9. P.G. de Gennes, Langmuir **12**, 4497 (1996).
10. R.A. Schapery, Int. J. Fract. **11**, 141; 369 (1975); **39**, 163 (1989).
11. J.A. Greenwood, K.L. Johnson, Philos. Mag. A **43**, 697 (1981).
12. M. Barber, J. Donley, J.S. Langer, Phys. Rev. A **40**, 366 (1989).
13. J.M. Baney, C.Y. Hui, J. Appl. Phys. **86**, 4232 (1999); C.Y. Hui, J.M. Baney, E.J. Kramer, Langmuir **14**, 6570 (1998).
14. B.N.J. Persson, E.A. Brener, Phys. Rev. E **71**, 036123 (2005).
15. G.I. Barenblatt, Adv. Appl. Mech. **7**, 55 (1962).
16. E.E. Gdoutos, P.M. Schubel, I.M. Daniel, Strain **40**, 119 (2004).
17. J.T. South, S.W. Case, K.L. Reifsnider, Mech. Mater. **34**, 451 (2002).

18. K. Tsunoda, J.J.C. Busfield, C.K.L. Davies, A.G. Thomas, J. Mater. Sci. **35**, 5187 (2000).
19. B.N.J. Persson, in preparation.
20. A.A. Griffith, Philos. Trans. R. Soc. London, A **221**, 163 (1920).
21. T.L. Anderson, *Fracture Mechanics: Fundamentals and Applications* (CRC Press, Boca Raton, 1995).
22. R.M. Christensen, Int. J. Fract. **15**, 3 (1979).
23. R.M. Christensen *Theory of Viscoelasticity*, 2nd edition (Dover Publications, Inc., Mineola, New York, 2003).
24. A.G. Thomas, J. Polym. Sci. **18**, 177 (1955).
25. A similar approach has already been applied successfully to rubber friction on rough substrates, where the flash temperature has a profound influence on the friction dynamics (B.N.J. Persson, unpublished).
26. K.L. Johnson, in V.V. Tsukruk, K.J. Wahl (Editors), *Microstructure and Microtribology of Polymer Surfaces* (American Chemical Society, Washington, DC, 2000) pp. 24-41.
27. K.N.G. Fuller, P.G. Fox, J.E. Field, Proc. R. Soc. London, Ser. A **341**, 537 (1975).
28. P.G. Fox, Soria-Ruiz, Proc. R. Soc. London, Ser. A **317**, 79 (1970).
29. R.D. Deegan, P.J. Petersan, M. Marder, H.L. Swinney, Phys. Rev. Lett. **88**, 014304 (2002); P.J. Petersan, R.D. Deegan, M. Marder, H.L. Swinney, Phys. Rev. Lett. **93**, 015504 (2004).
30. L.B. Freund, *Dynamical Fracture Mechanics* (Cambridge University Press, Cambridge, 1990).
31. M. Marder, Phys. Rev. Lett. **94**, 048001 (2005).
32. B.N.J. Persson, Phys. Rev. Lett. **81**, 3439 (1998); J. Phys. C **10**, 10529 (1998); J. Chem. Phys. **110**, 9713 (1999).
33. D.S. Dugdale, J. Mech. Phys. Solids **8**, 100 (1960).
34. A.D. Roberts, A.G. Thomson, Wear **33**, 45 (1975).
35. F. Lacroix, A. Tougui, N.R. Neelakantan, N. Ranganathan, *A new approach for crack growth life of an elastomeric material*, in *The 15th European Conference of Fracture-Advanced Fracture Mechanics for Life and Safety Assessments, Stockholm, Sweden, August 11-13, 2004.*